

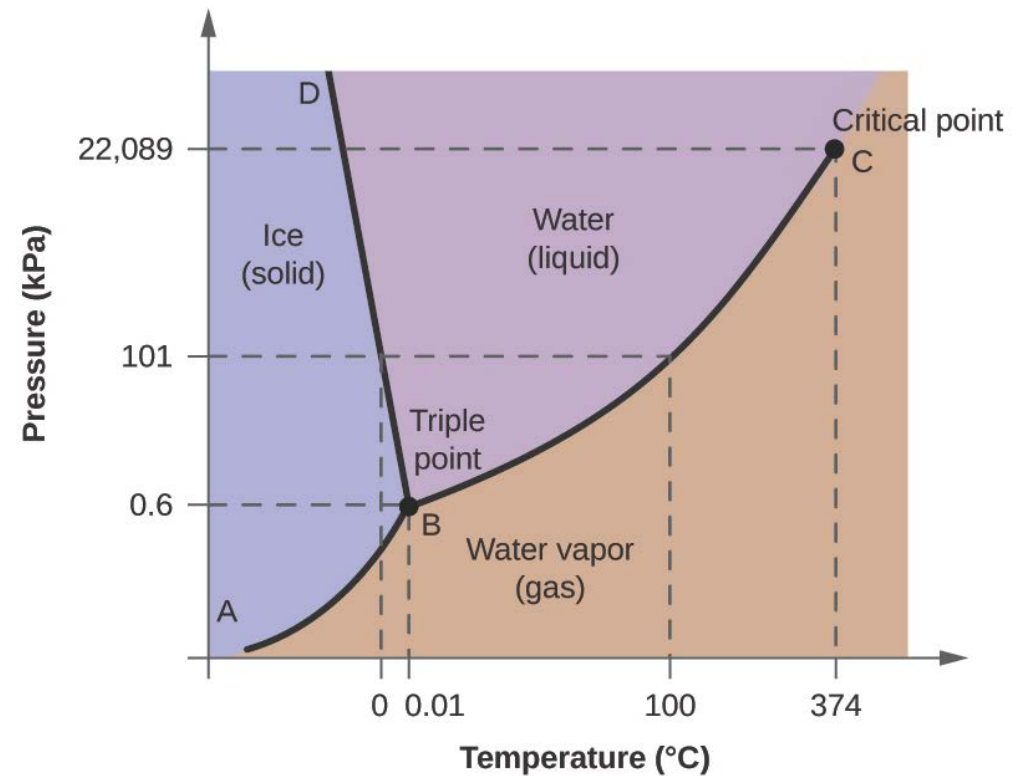
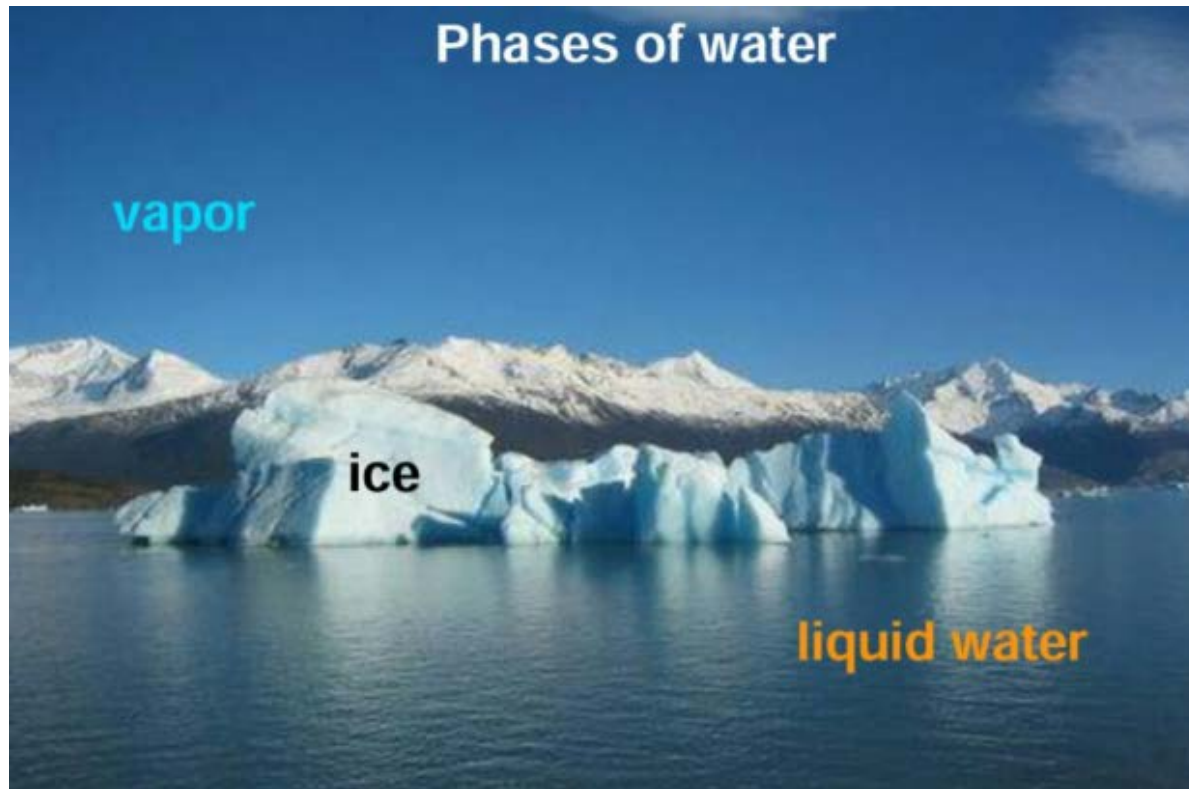
Exploring strangeness:
 Λ baryon production in heavy-ion collisions
with NA61/SHINE experiment

Yuliia Balkova (University of Silesia in Katowice)



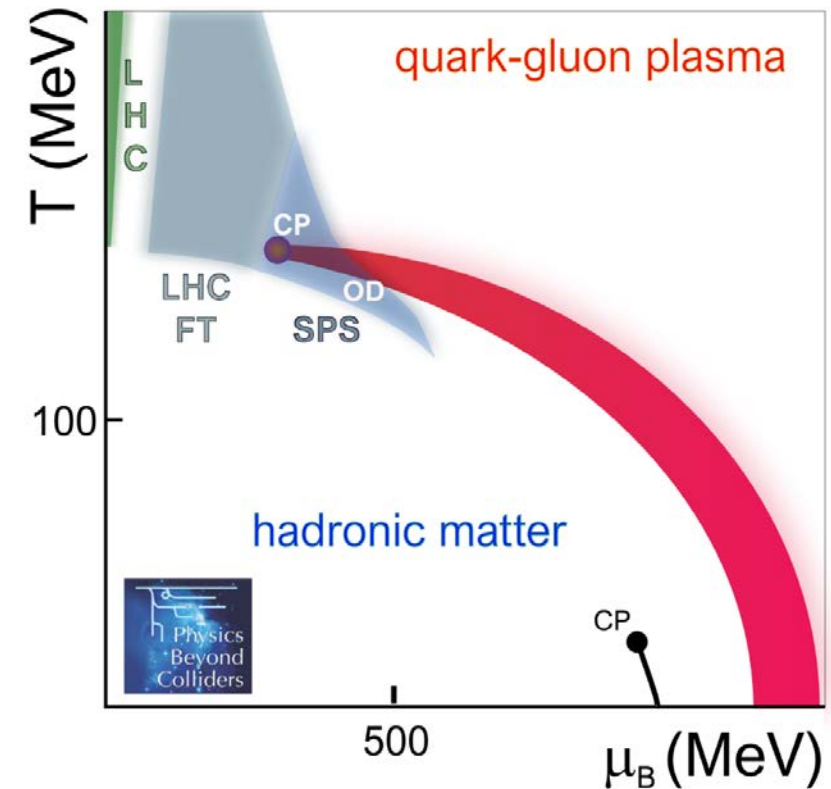
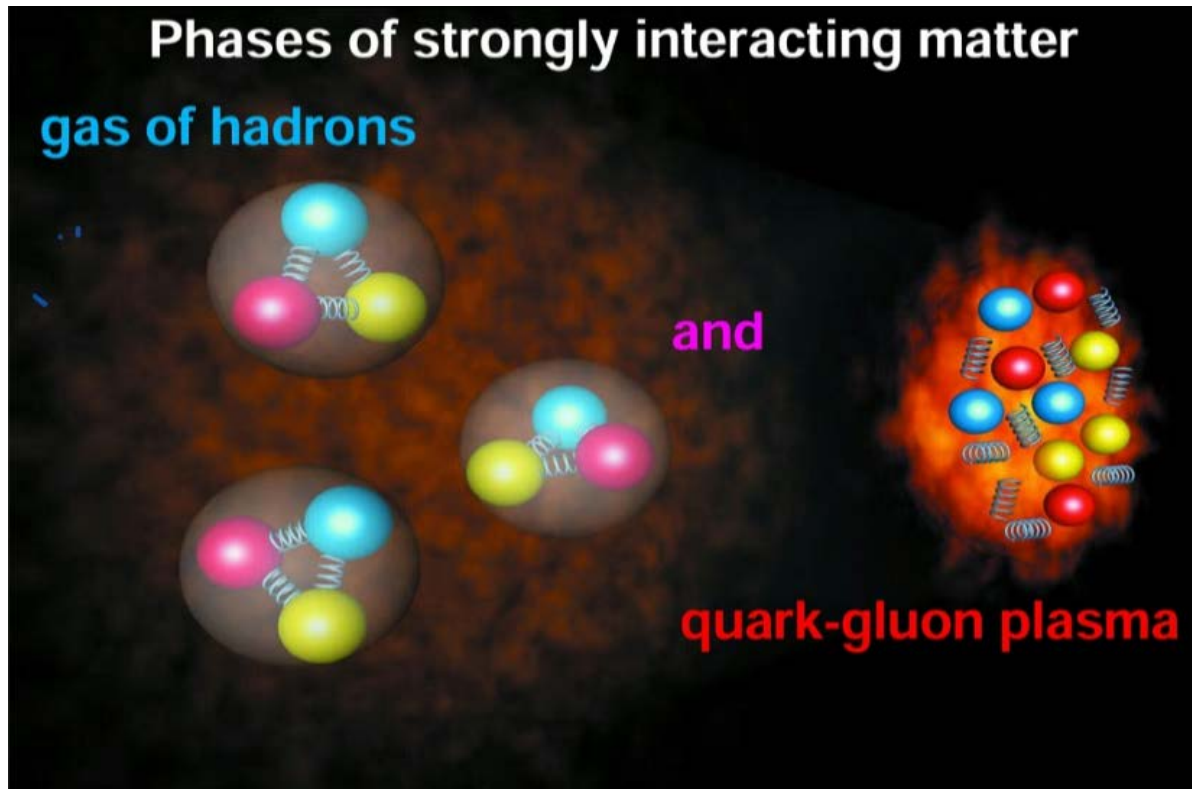
Well-known example – phase diagram of water

- **phase diagram** is a plot, which contains information about conditions at which thermodynamically distinct phases occur and coexist at equilibrium.



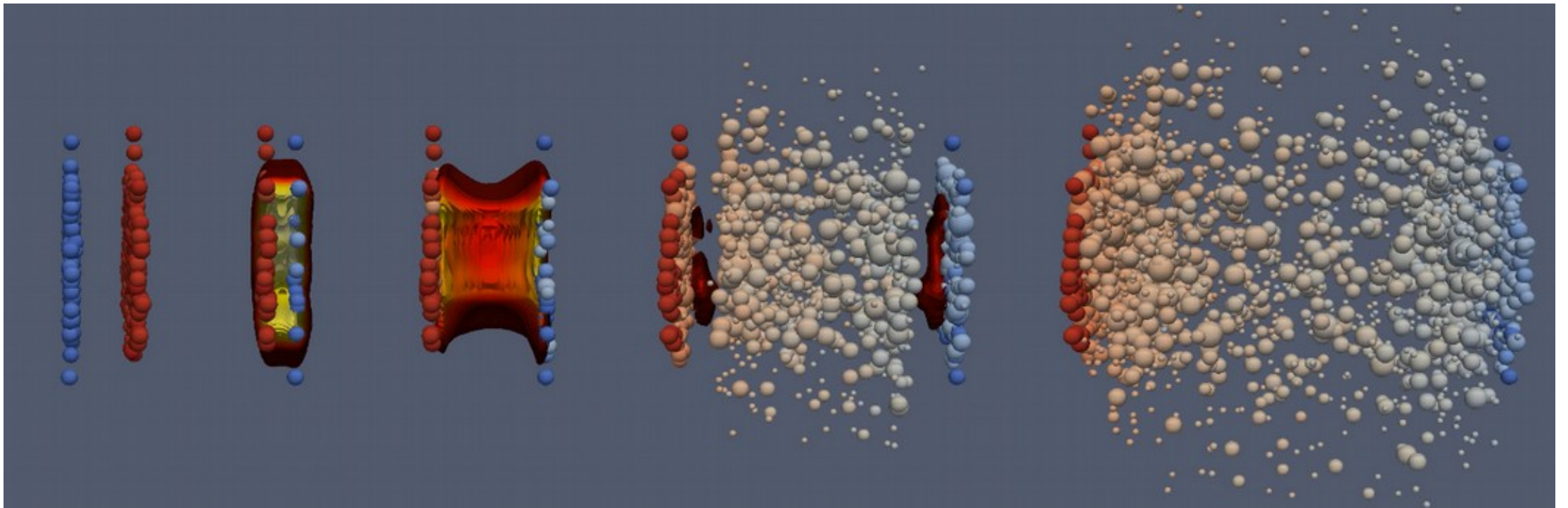
Phase diagram of strongly interacting matter

- what if the same will be done for the nuclear matter?



Quark-gluon plasma

- QGP is a state of the nuclear matter when quarks are **deconfined** (or freed) of their strong attraction, which is believed to constitute the early Universe and neutron stars
- laboratory setup: **heavy-ion collisions**



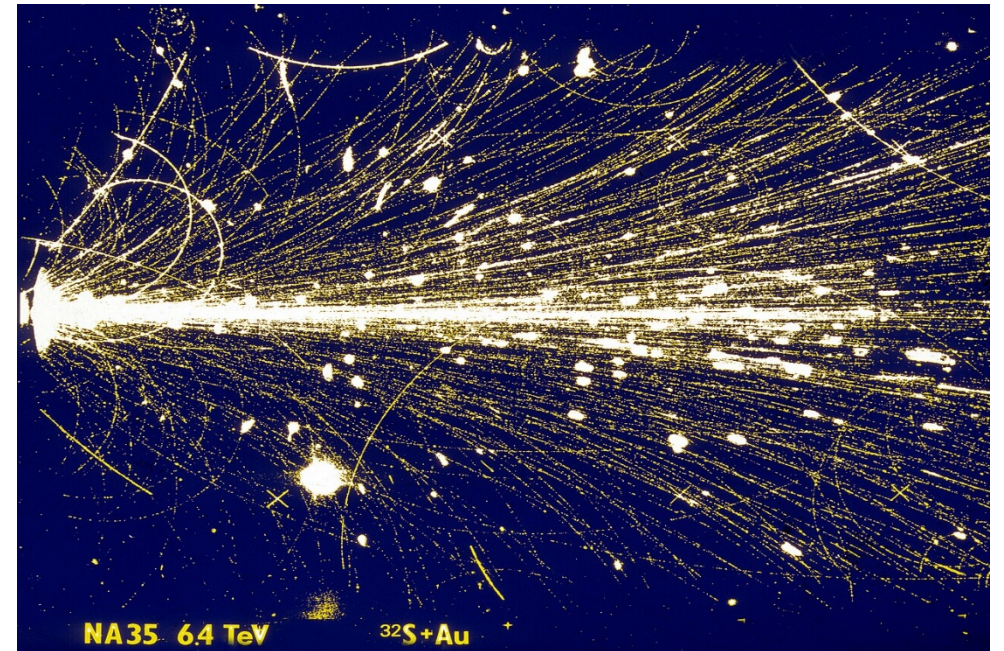
Quark-gluon plasma: signatures

predicted theoretically:

- dilepton/photon QGP radiation (E.V. Shuryak, Phys. Rept., vol. 61, pp. 71–158, 1980)
- strangeness enhancement (J. Rafelski and B. Muller, Phys. Rev. Lett., vol. 48, p. 1066, 1982)
- J/ψ suppression (T. Matsui and H. Satz, Phys. Lett., vol. B178, pp. 416–422, 1986)

and confirmed experimentally with:

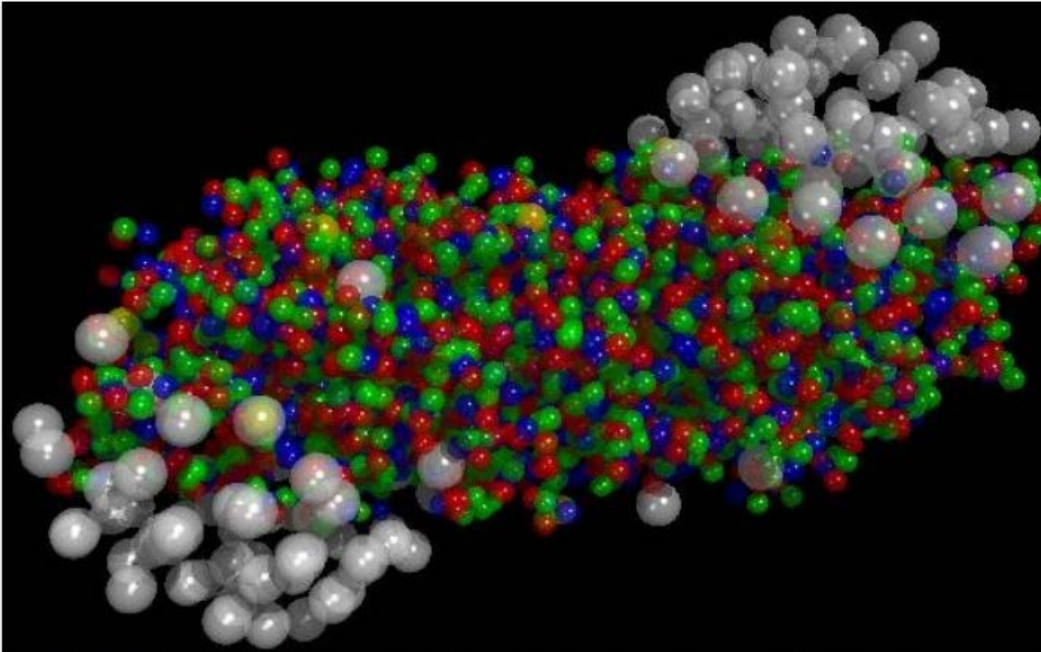
- O and S beams at 200A GeV (NA34-2, NA35, NA36, NA38, WA80, WA85 and WA94 at CERN SPS)
- Pb and In beams at 158A GeV (NA44, NA45, NA49, NA50, NA52, NA57, NA60, WA97 and WA98 at CERN SPS)



Quark-gluon plasma: announcement and aftermath

New State of Matter created at CERN

10 February, 2000



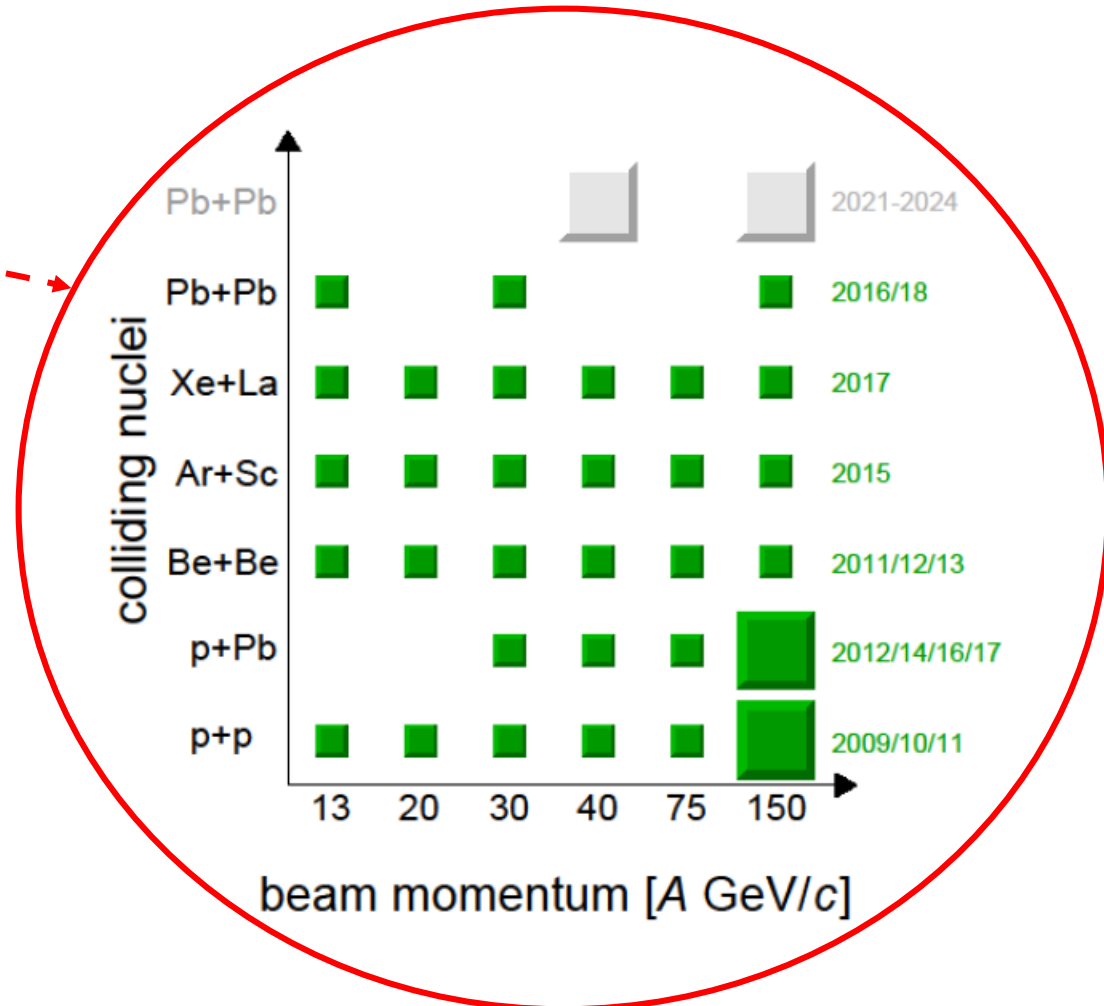
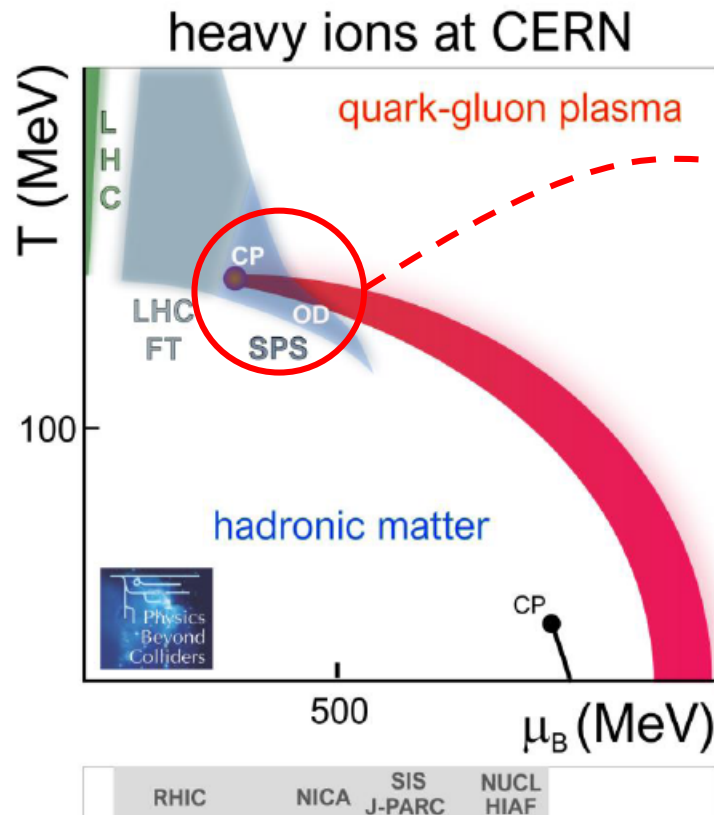
Geneva, 10 February 2000. At a special seminar on 10 February, spokespersons from the experiments on CERN¹'s Heavy Ion programme presented compelling evidence for the existence of a new state of matter in which quarks, instead of being bound up into more complex particles such as protons and neutrons, are liberated to roam freely.

Two main pursuits in the heavy-ion community:

- properties of high-temperature QGP (high energies at RHIC, LHC)
- search for the onset of deconfinement (collision system scan at CERN SPS)

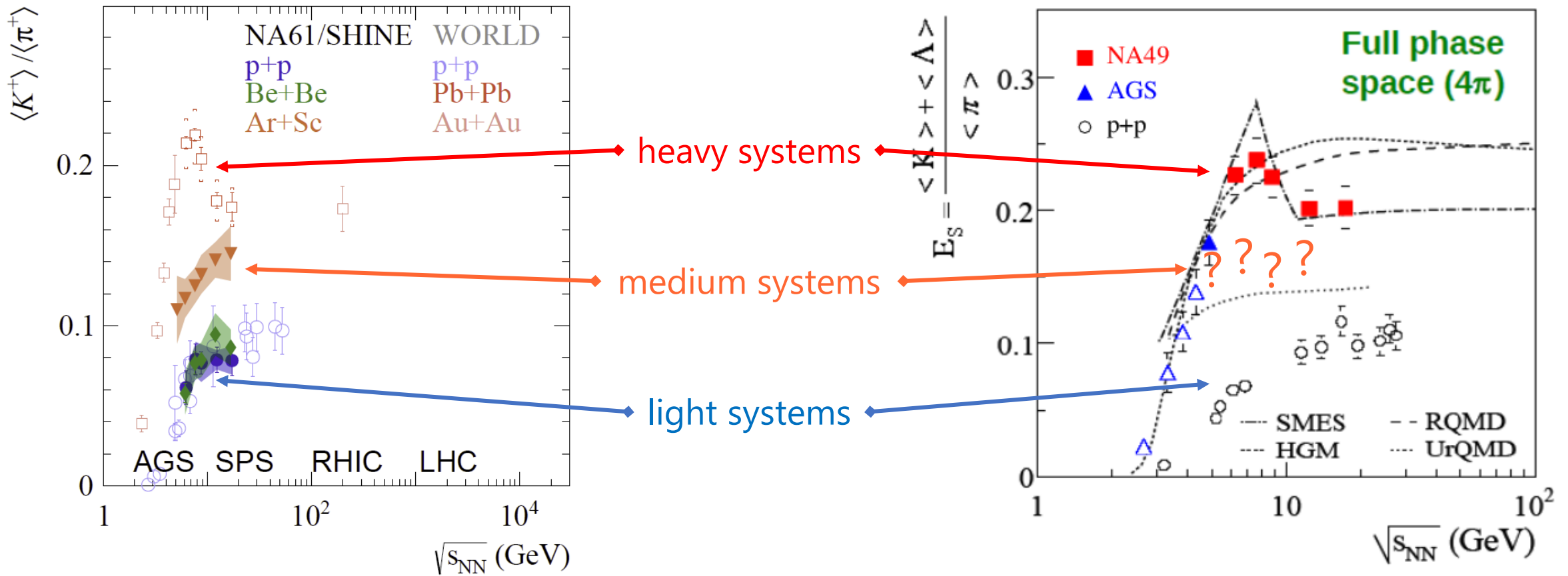
NA61/SHINE two-dimensional scan

NA61/SHINE performed the 2D scan in collision energy and system size to study the phase diagram of strongly interacting matter.



Onset of deconfinement: horn

Rapid changes in strangeness production E_s („horn“) were observed in **Pb+Pb** collisions at SPS energies by NA49, which was predicted as a signature of the **onset of deconfinement**. On the contrary, a plateau-like structure is visible in **p+p** and **Be+Be**.

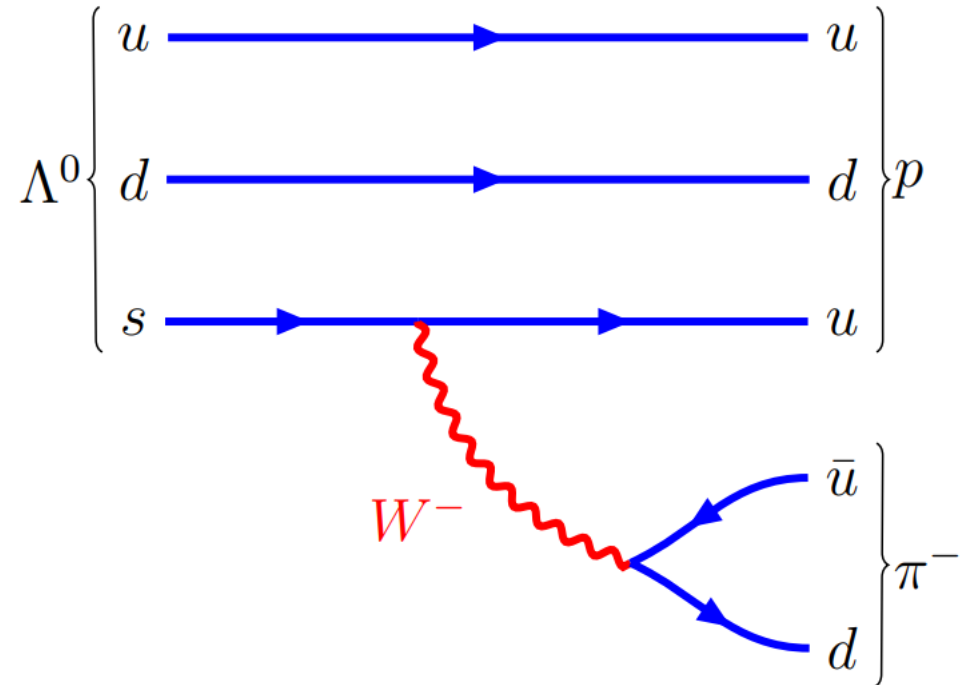


General plan for my analysis

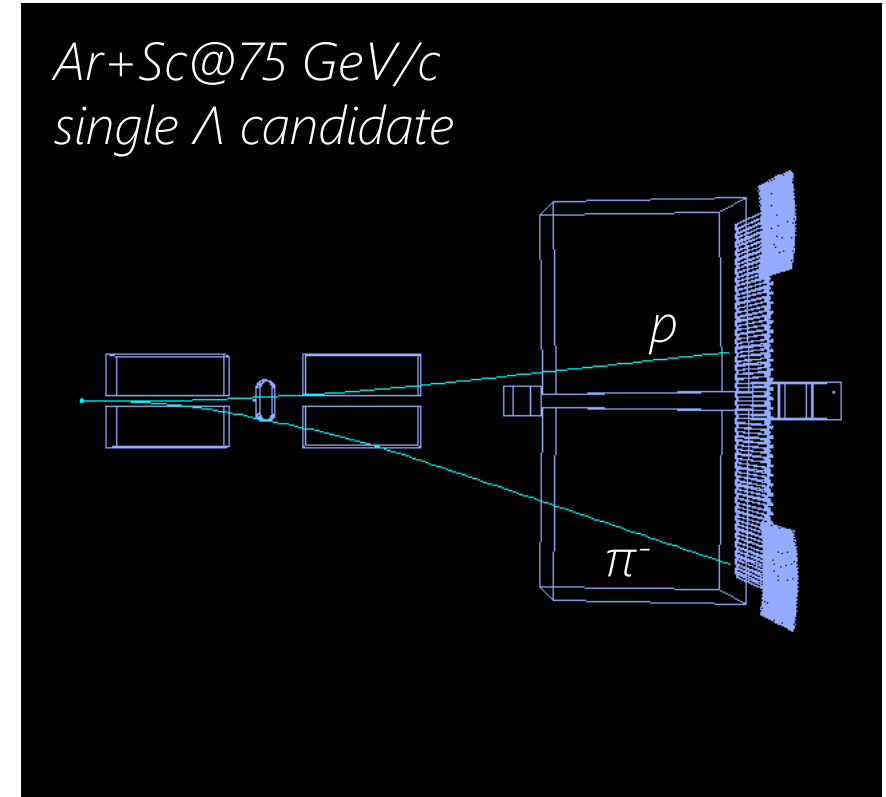
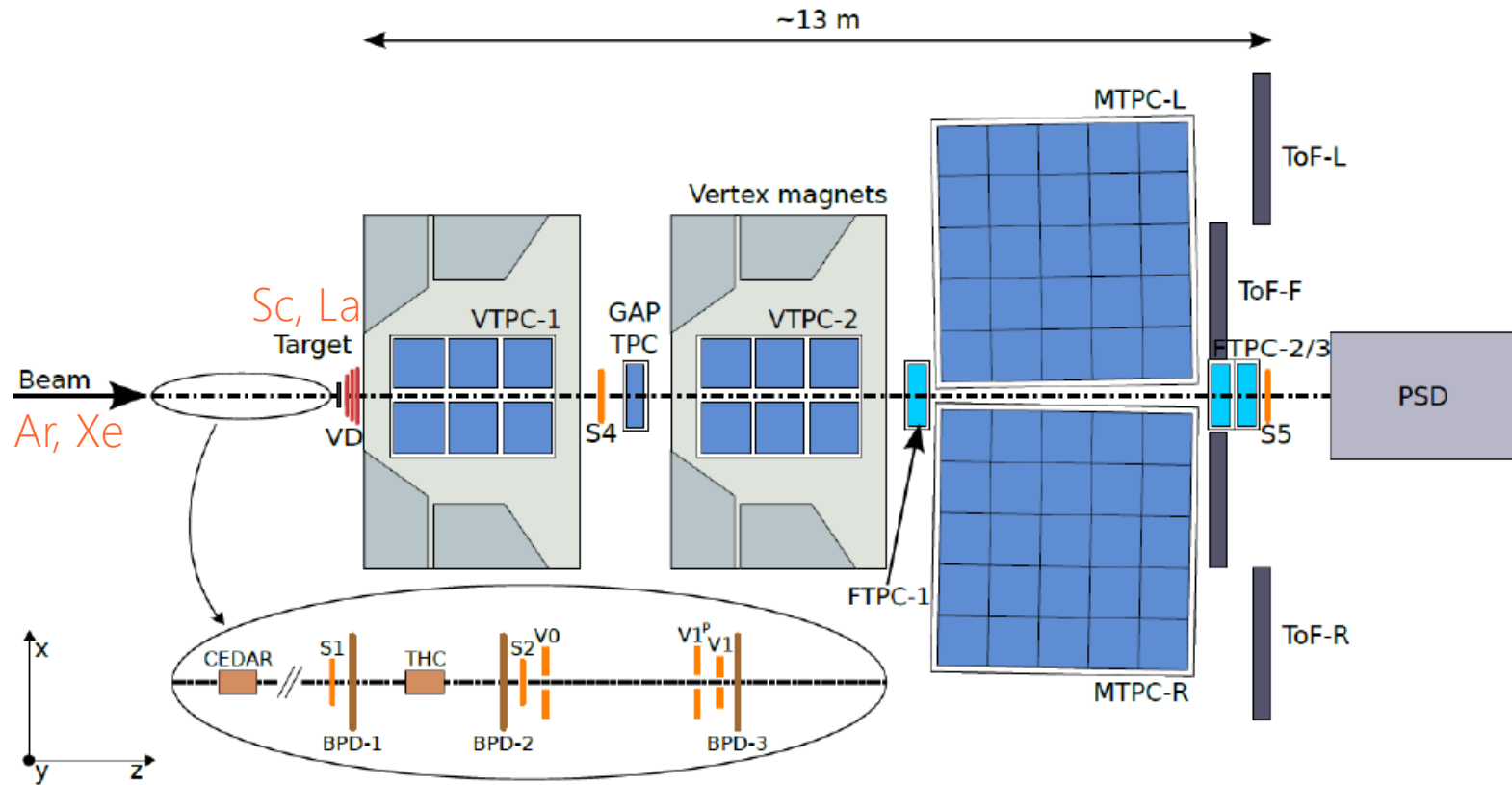
The main goal is to measure Λ baryon production in **Ar+Sc** and then **Xe+La** interactions at CERN SPS energy range.

Properties of Lambda baryon [[PDG](#)]:

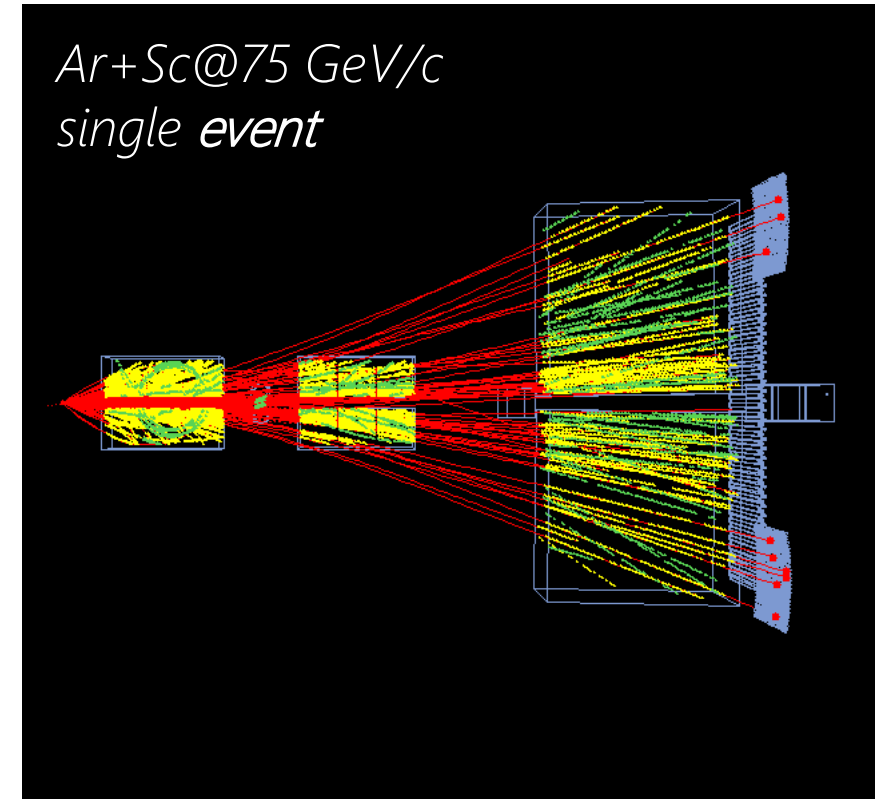
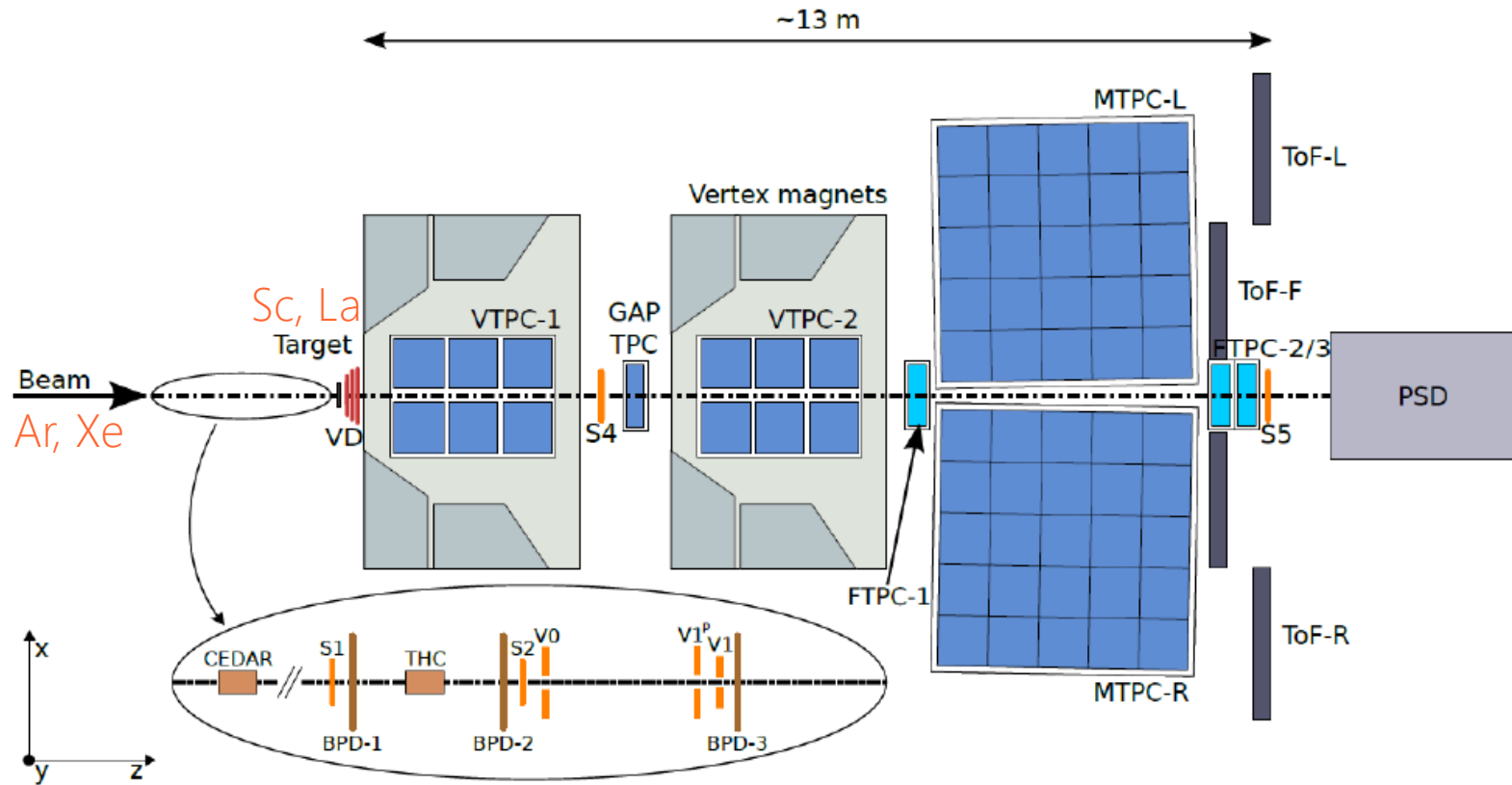
- rest mass $m = 1115.683 \pm 0.006 \text{ MeV}$
- mean lifetime $\tau = (2.632 \pm 0.020) \times 10^{-10} \text{ s}$
 - $c\tau = 7.89 \text{ cm}$
- decay modes
 - $p\pi^- \quad \Gamma_i/\Gamma = (63.9 \pm 0.5) \%$
 - $n\pi^0 \quad \Gamma_i/\Gamma = (35.8 \pm 0.5) \%$



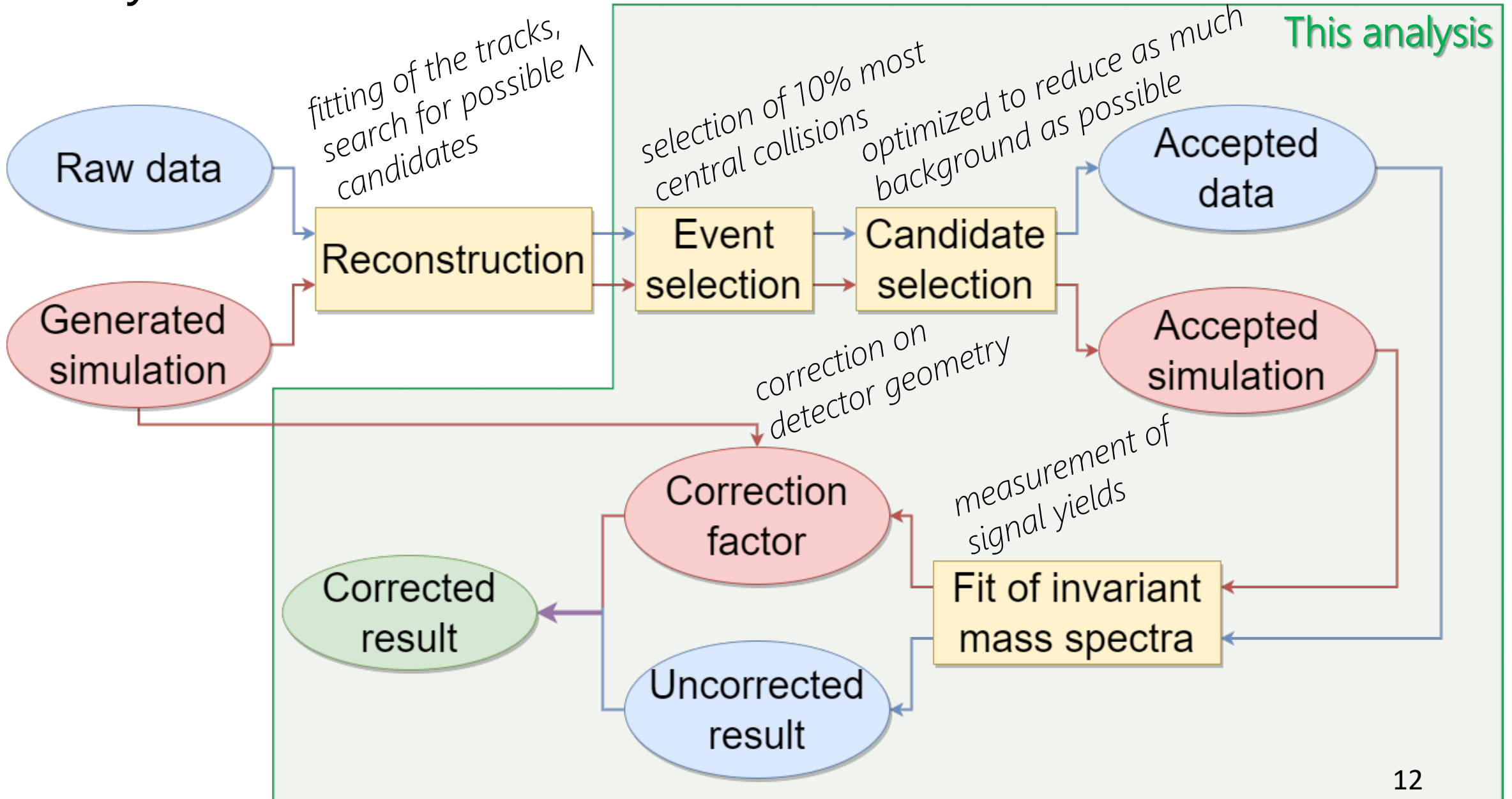
Schematic layout of the NA61/SHINE experiment



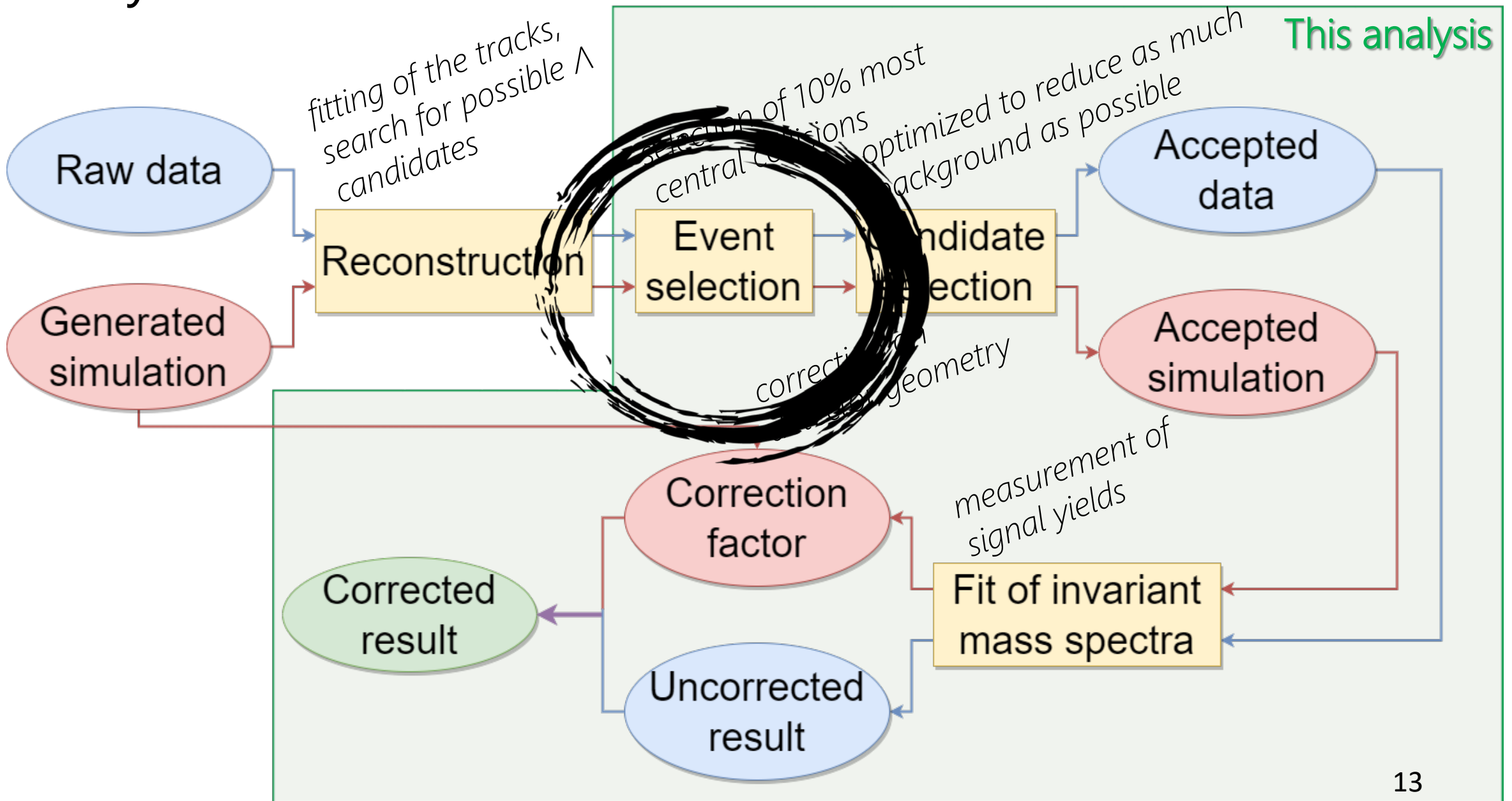
Schematic layout of the NA61/SHINE experiment



Analysis workflow



Analysis workflow



Event selection

The subsample of data, which consists of central interactions of Ar beam ions with Sc target nuclei, is selected on the **trigger** level. To subsequently ensure good quality of the data, the following event selection criteria were imposed:

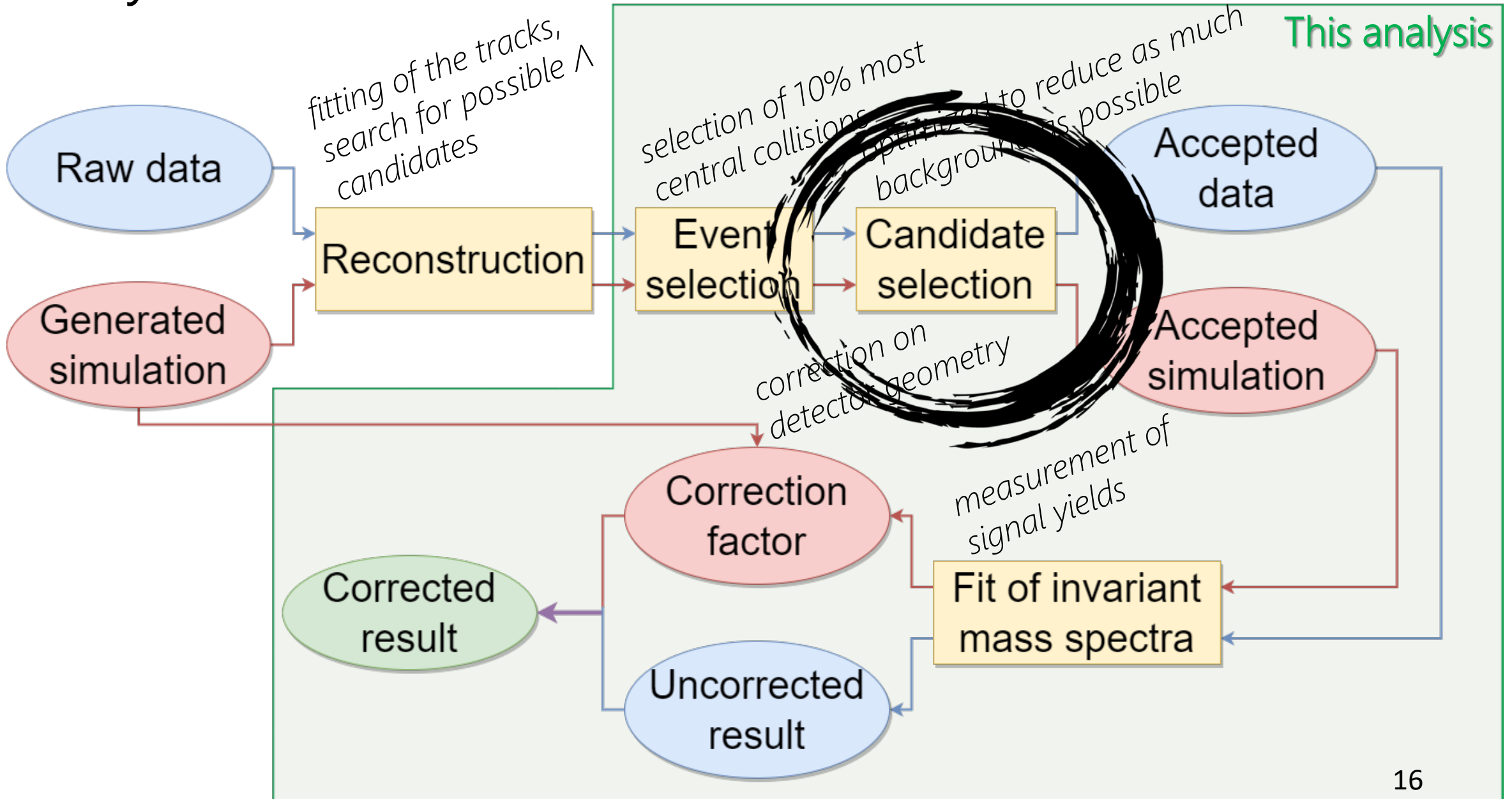
- no off-time beam particle was detected within a time window of $\pm 4 \mu\text{s}$ around the trigger particle,
- no other interaction trigger was detected within a time window of $\pm 25 \mu\text{s}$ around the trigger particle,
- beam particle was detected in at least three planes out of four of BPD-1 and BPD-2 and in both planes of BPD-3,
 - a well-reconstructed interaction vertex with z-coordinate (fitted using the beam trajectory and TPC tracks) not farther away than 2 cm from the center of the Sc target,
 - an upper limit on the measured energy in PSD (number of spectators in MC), selecting 10% of most central collisions.

Event selection

Event statistics in experimental data available for the analysis:

ρ_{beam}	40A GeV/c ($\sqrt{s_{NN}} = 8.77$ GeV)	75A GeV/c ($\sqrt{s_{NN}} = 11.94$ GeV)	150A GeV/c ($\sqrt{s_{NN}} = 16.83$ GeV)
before selection	8.9M events	4.1M events	2.5M events
after selection	1.3M events	1.1M events	0.78M events

Analysis workflow

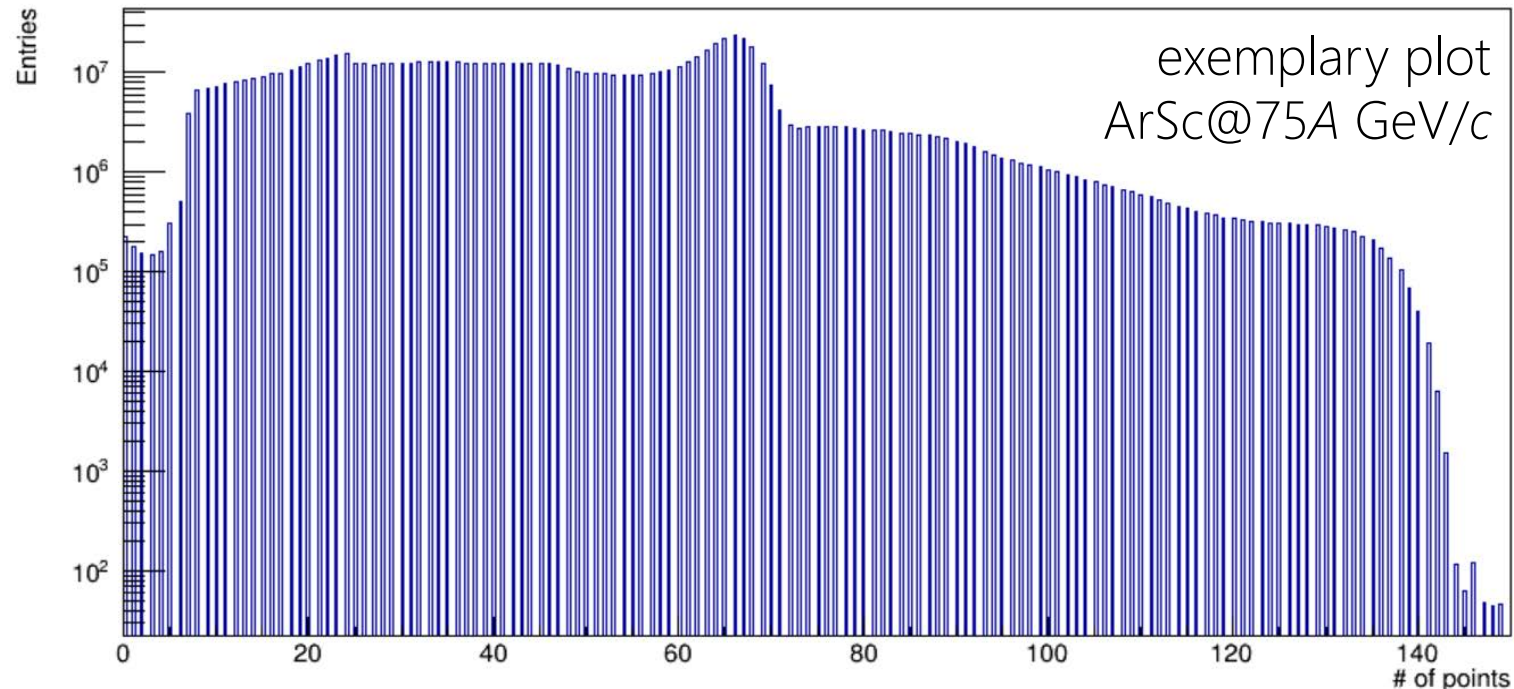


Track selection

The tracks which satisfy the following selection criteria were used in the analysis:

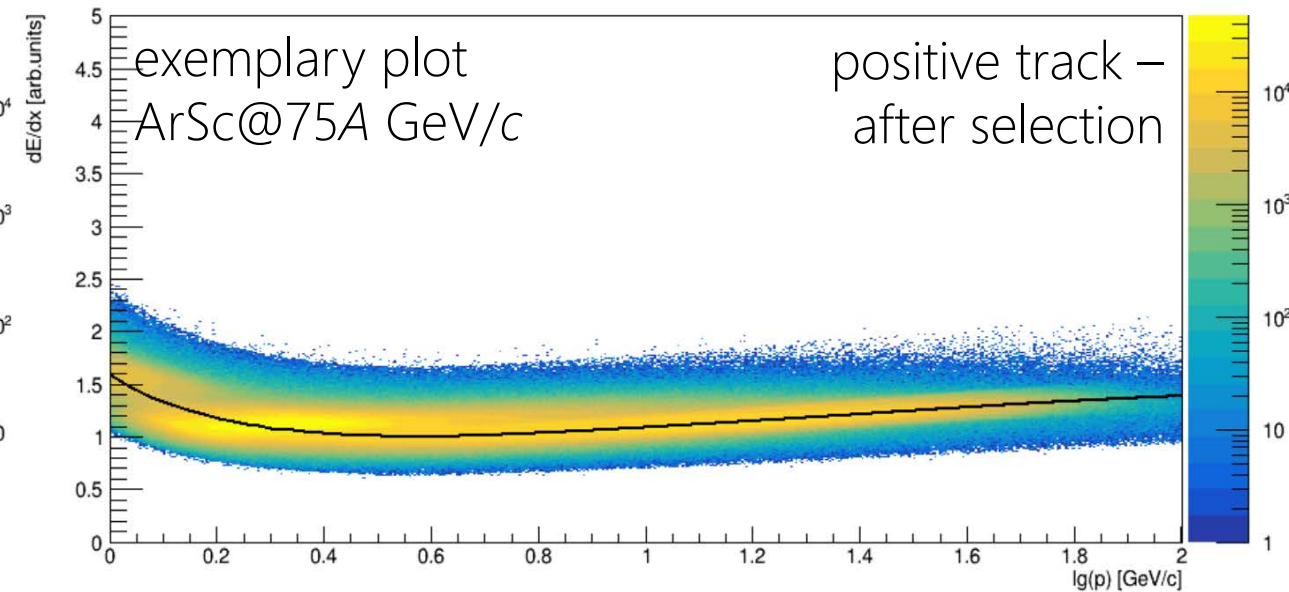
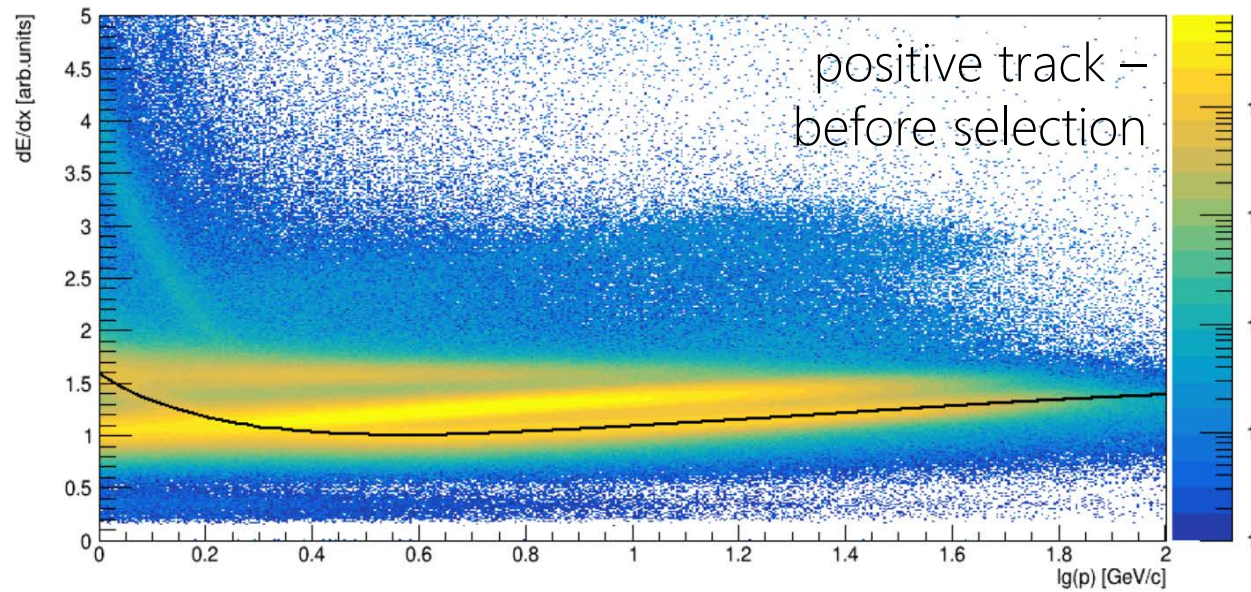
- the minimum number of measured clusters in both VTPCs was required to be 10 to ensure good momentum determination
- the minimum reconstructed momentum was required to be 0.5 GeV/c to reduce the background from electrons

Number of points in VTPC1+VTPC2 for first track



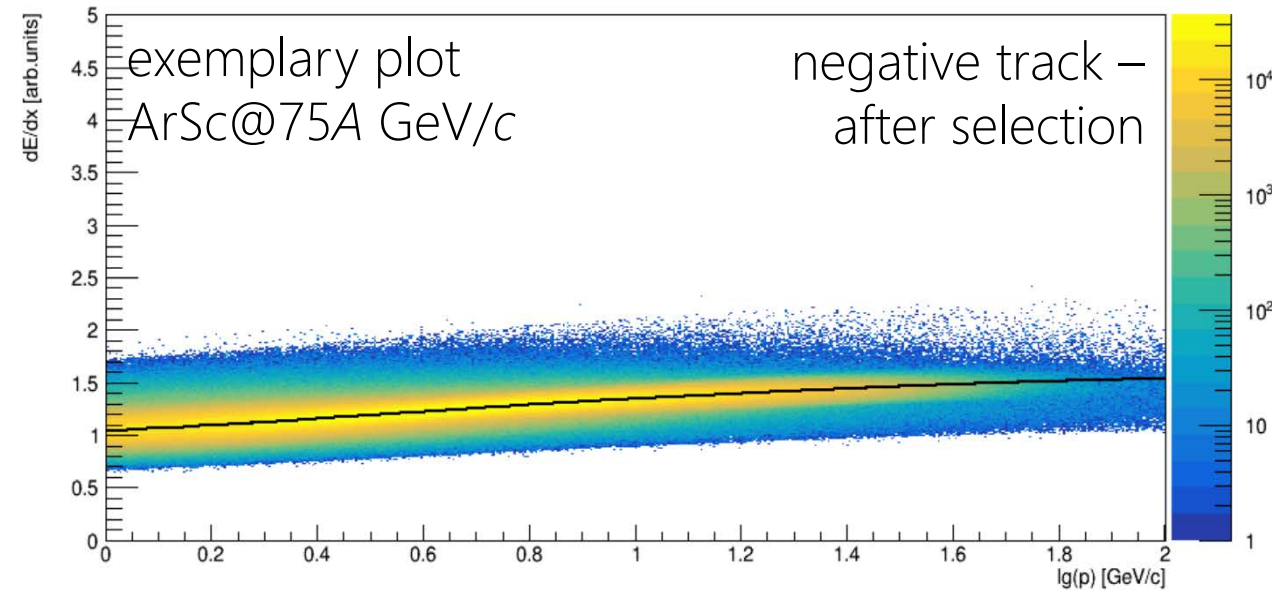
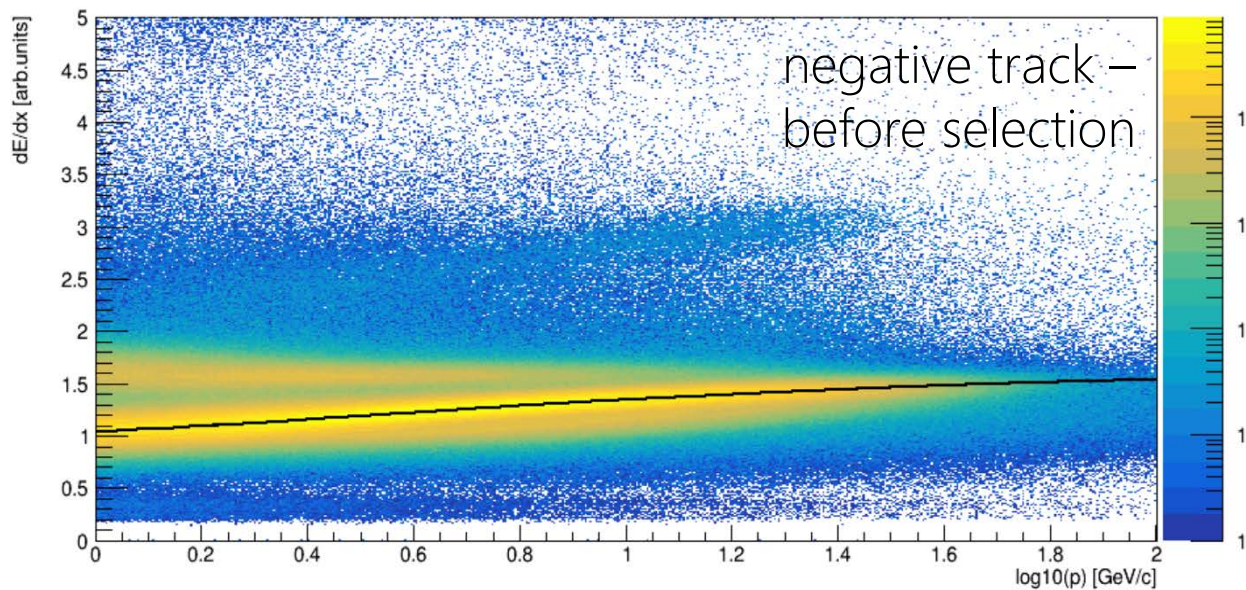
Candidate selection: PID through dE/dx method

- the proton candidates were selected by requiring their respective measured specific energy losses dE/dx to be within $\pm 3\sigma$ around the nominal Bethe-Bloch value



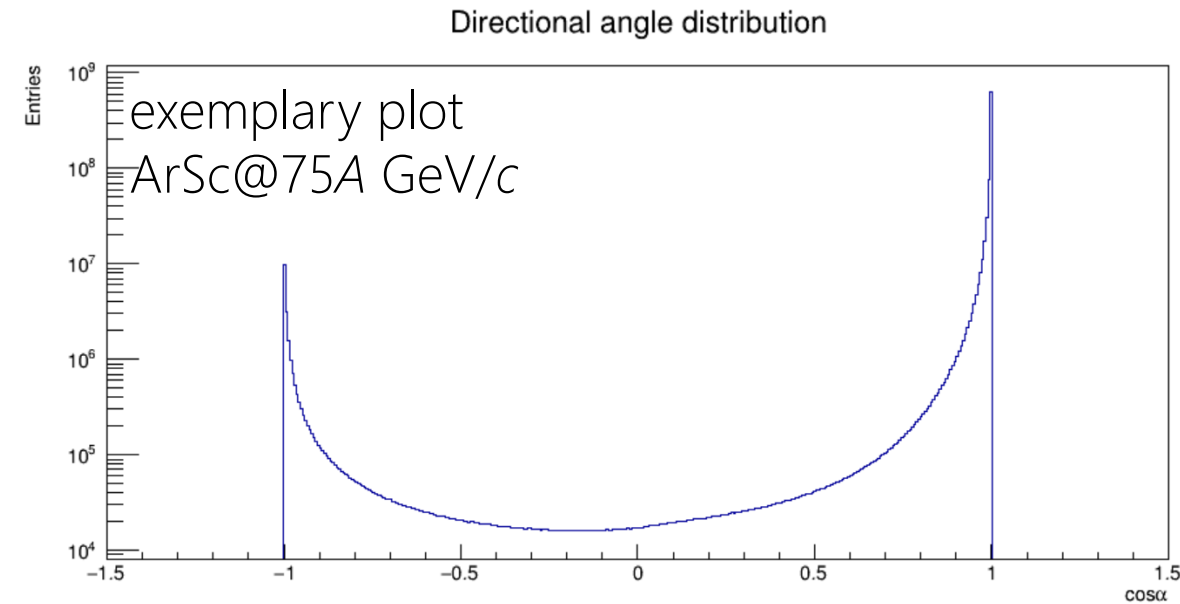
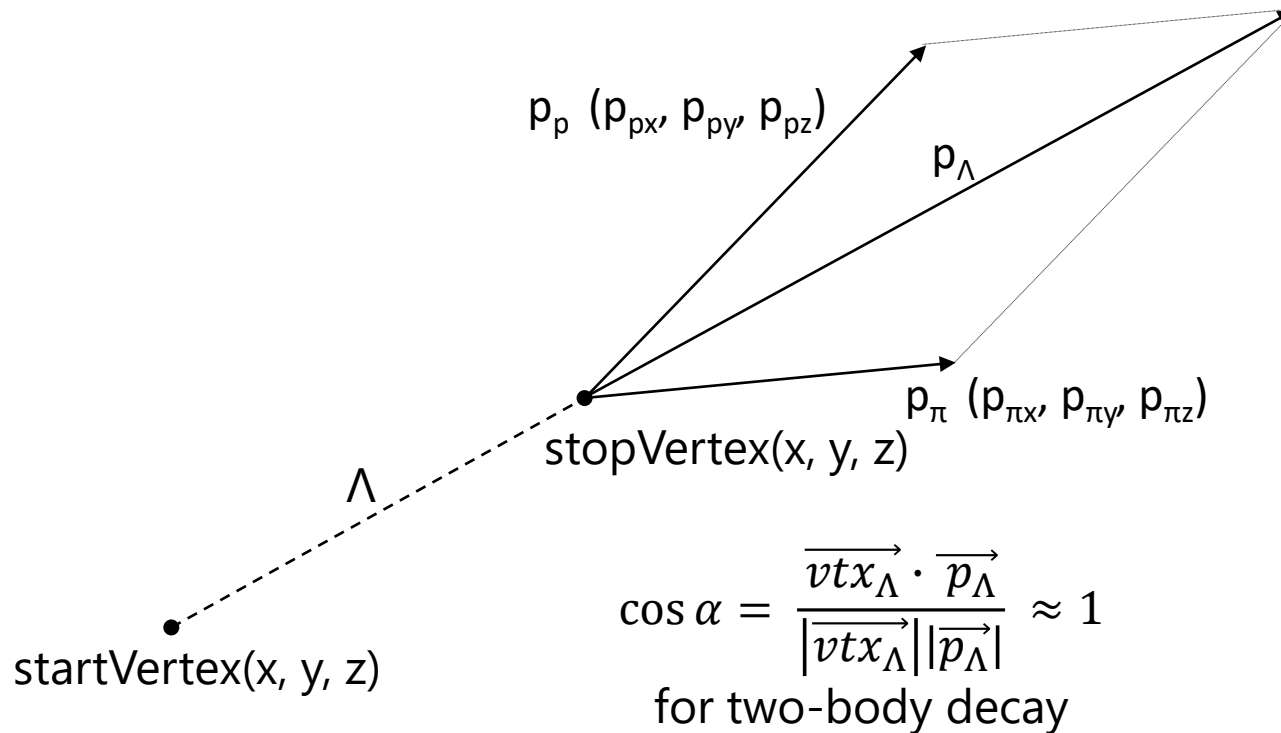
Candidate selection: PID through dE/dx method

- the pion candidates were selected by requiring their respective measured specific energy losses dE/dx to be within $\pm 3\sigma$ around the nominal Bethe-Bloch value



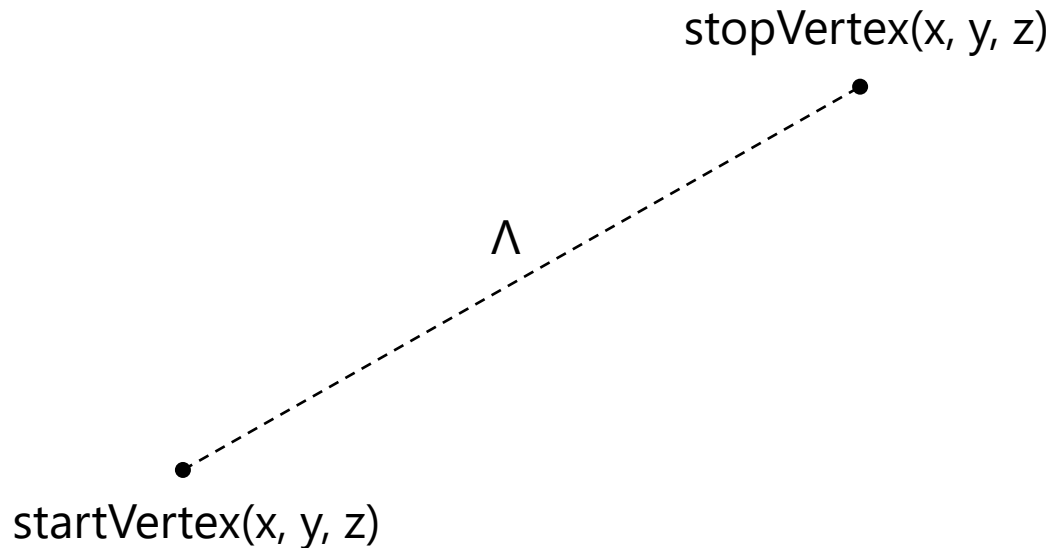
Candidate selection: cosine of directional angle (DirA)

- cosine of the angle between the sum of the 4-momentum of Lambda candidate decay products and a line connecting the primary production vertex and the Lambda candidate decay vertex
- the selection is rapidity-dependent and needs optimization

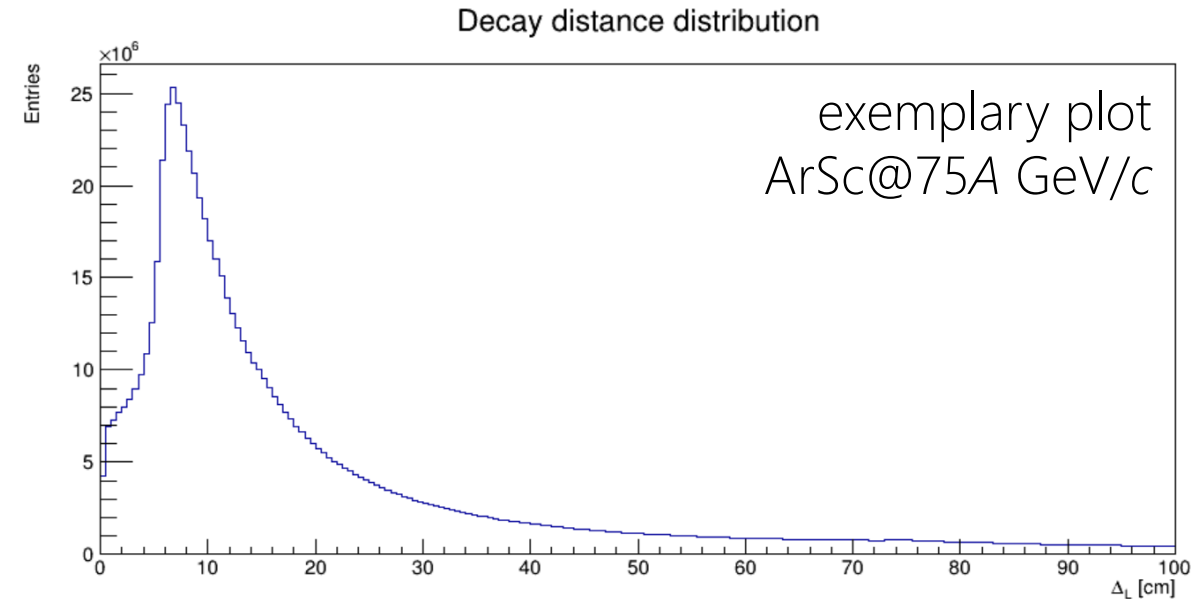


Candidate selection: decay distance ΔL

- distance between the primary production vertex and Lambda candidate decay vertex
- the selection is rapidity-dependent and needs optimization.



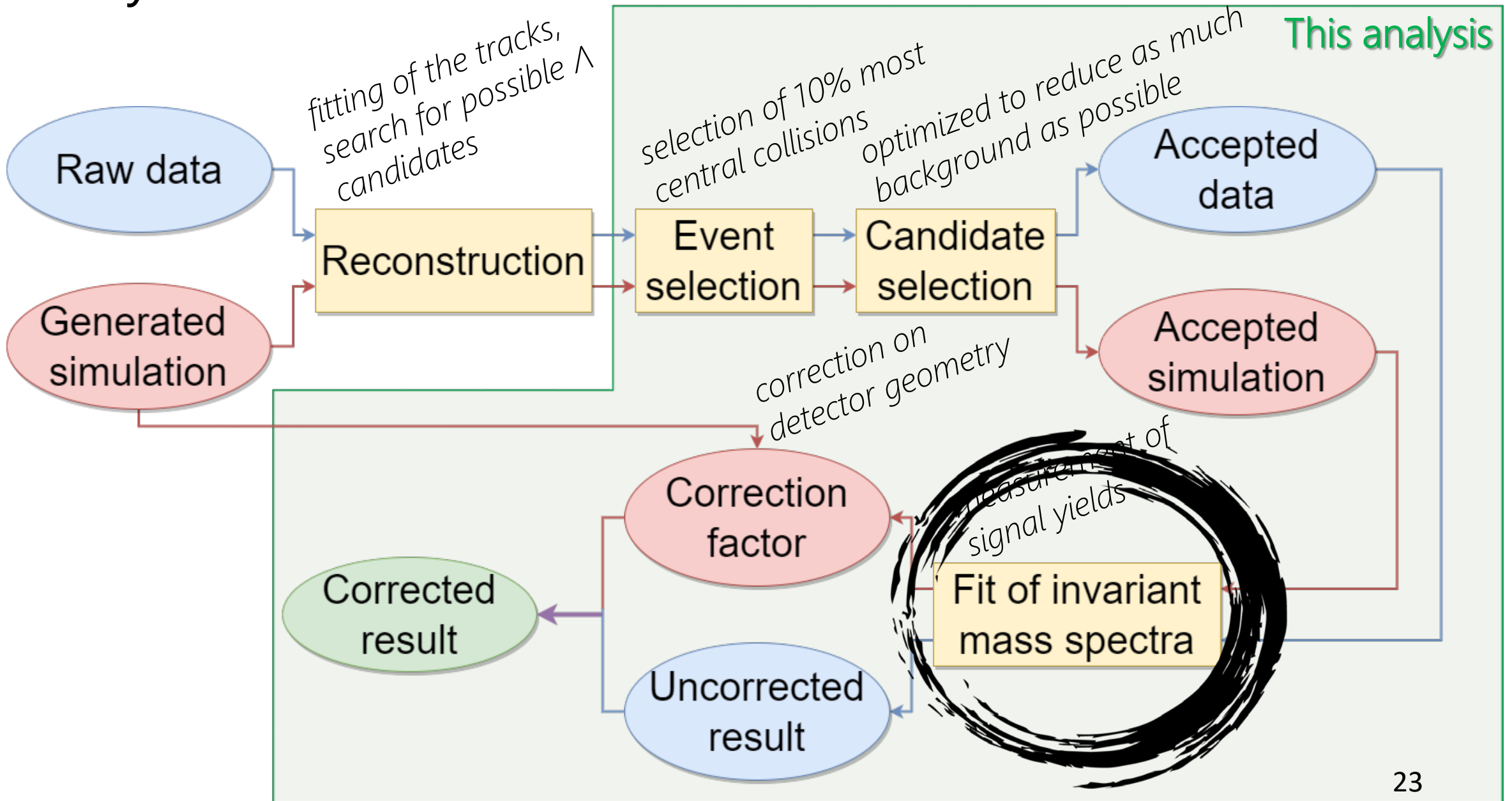
$$\Delta L = |\vec{L}| = \sqrt{\sum_{i=x,y,z} (startVertex_i - stopVertex_i)^2}$$



Selection optimization

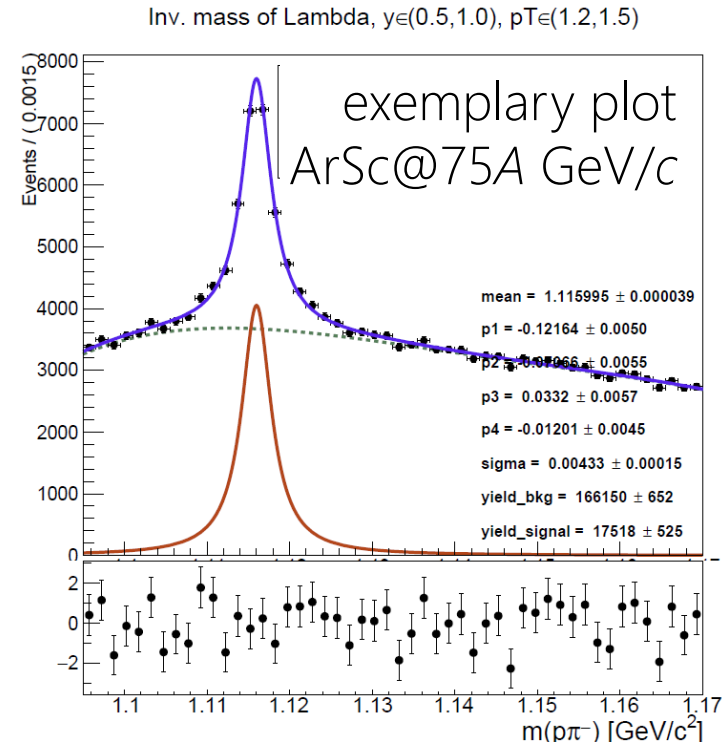
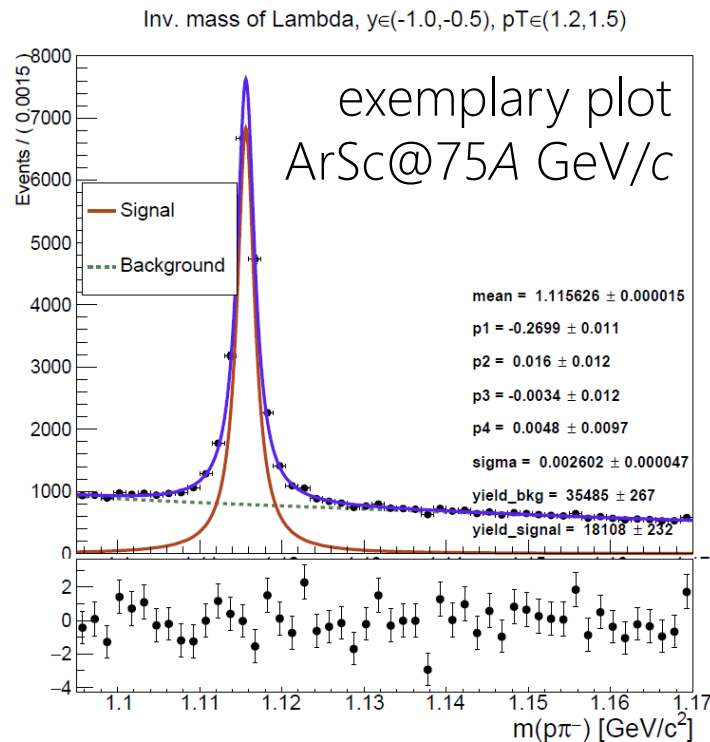
- is done on Monte-Carlo data (compared with experimental data)
- mass invariant spectrum is plotted for a given rapidity bin and given selection value
- obtained mass invariant spectra are fitted
- signal significance $S/\sqrt{S+B}$ is subsequently calculated for each selection value
- the optimal cut value for each rapidity bin is selected as the crossing with a signal decrease
- the stability of results is checked for all selection values

Analysis workflow

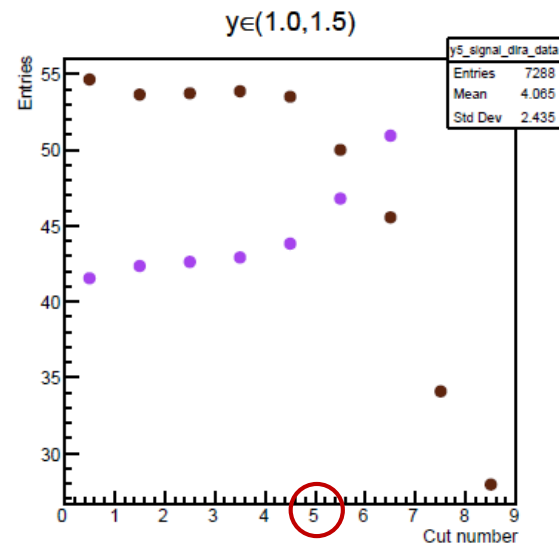
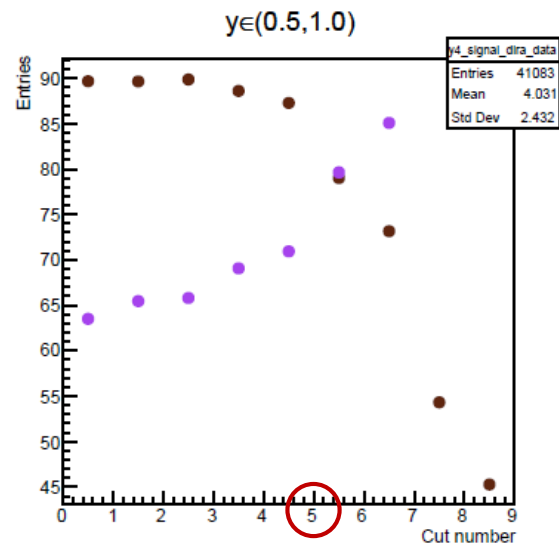
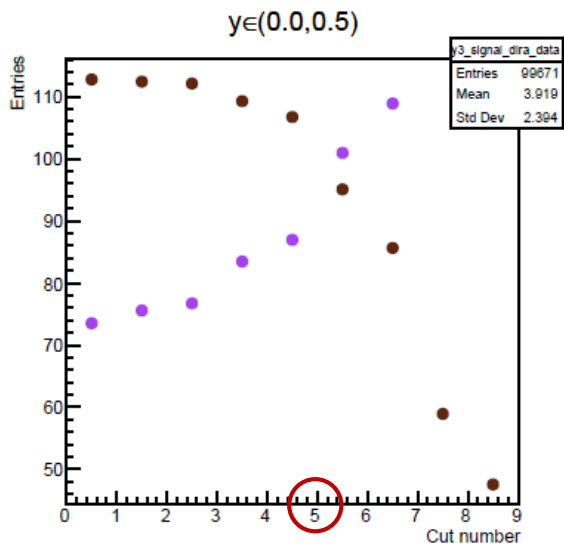
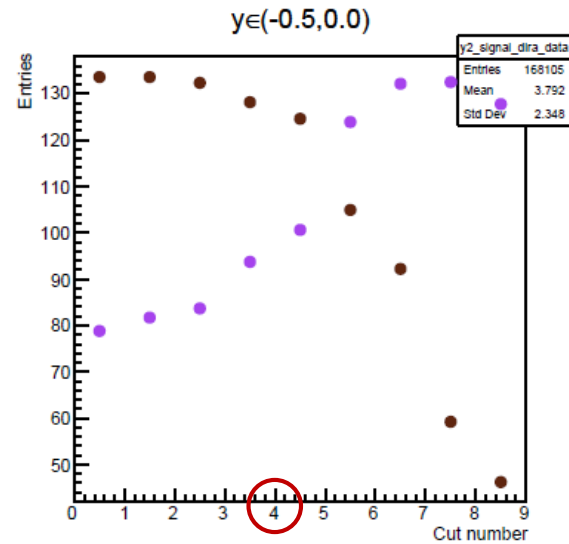
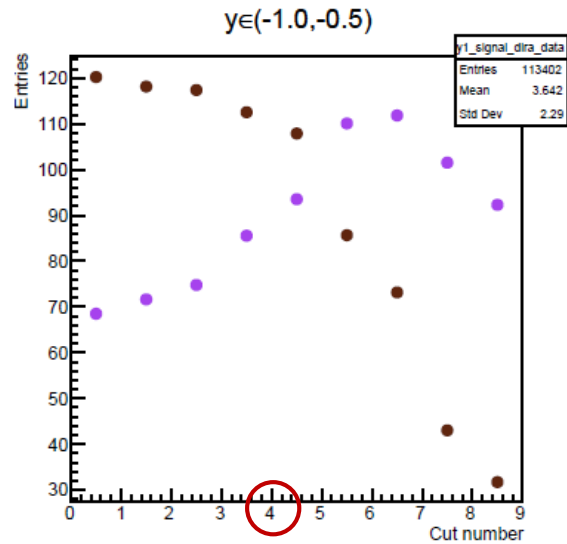
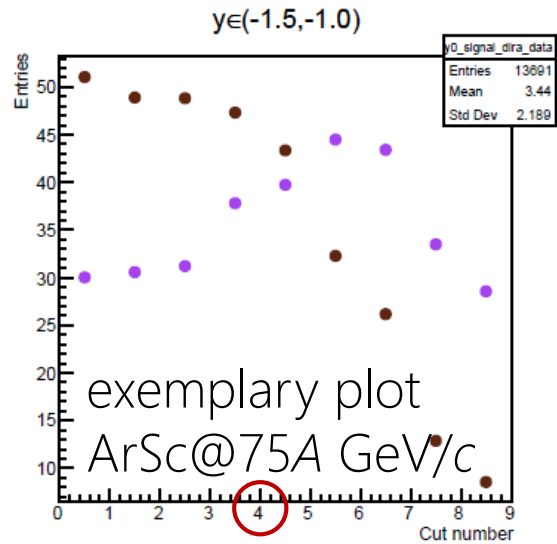


Fitting procedure

- number of selected signal Lambda candidates is estimated by fitting the invariant mass distribution
- signal is parametrized with a Breit-Wigner distribution
- background is parametrized with a 4th(3rd) order Chebychev polynomial
- the unbinned extended maximum likelihood method in RooFit is used



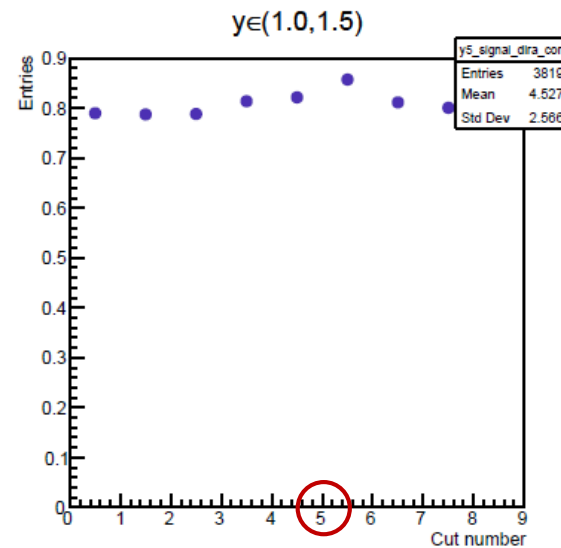
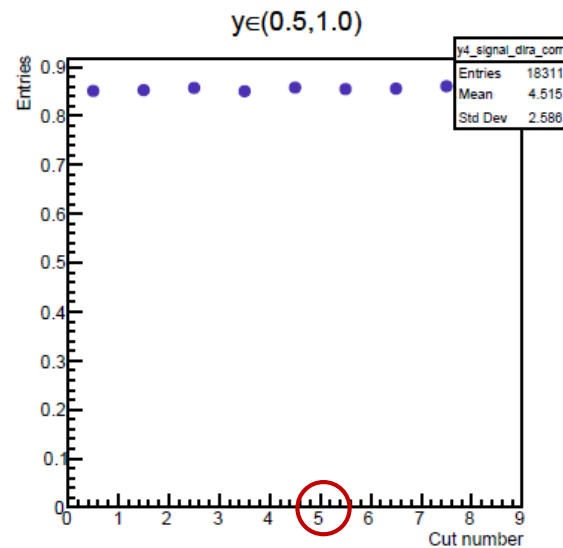
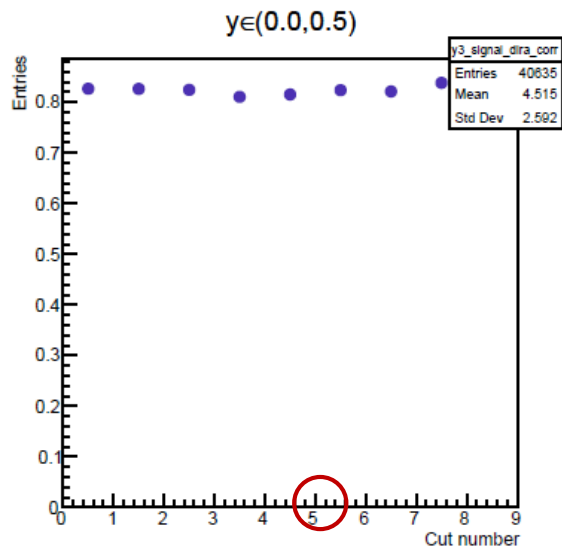
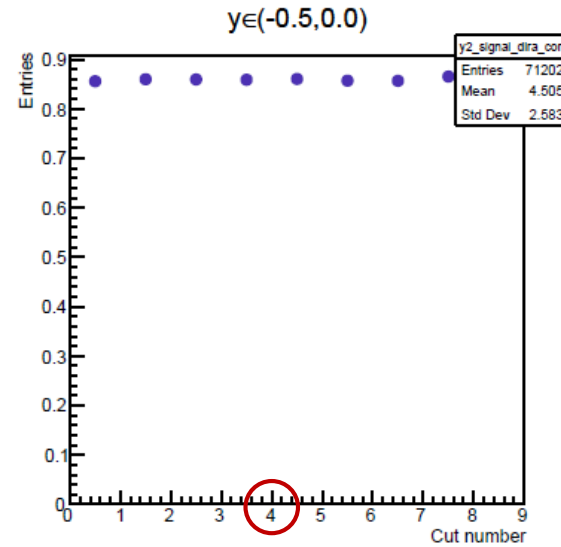
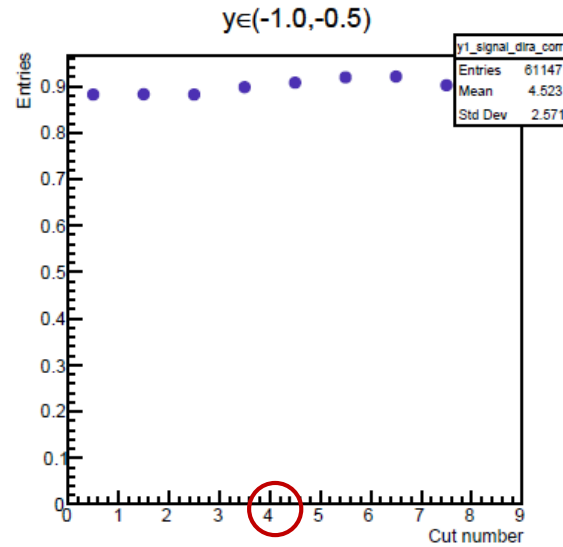
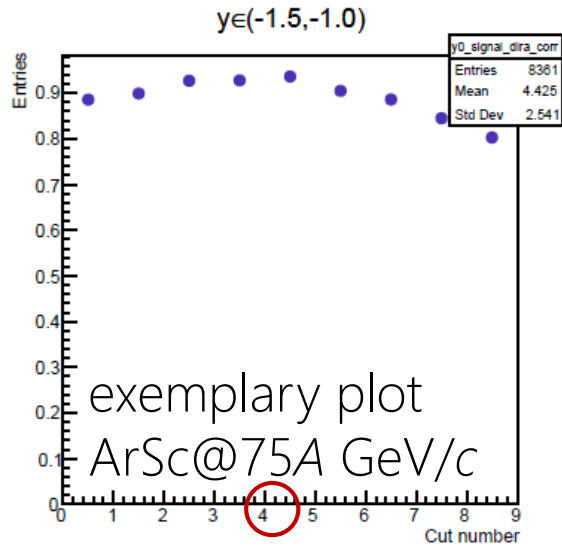
Signal significance for DirA selection



Cut number	DirA value
1	0.99
2	0.995
3	0.999
4	0.9995
5	0.9999
6	0.99995
7	0.99999
8	0.999995

$$SS = \frac{S_{sim}}{\sqrt{S_{sim} + B_{sim}}}$$

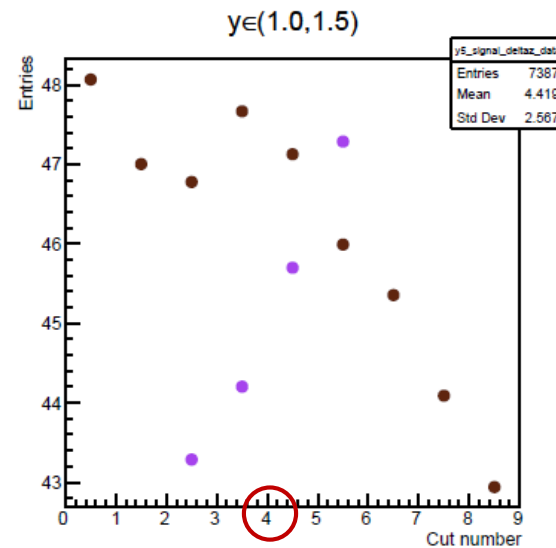
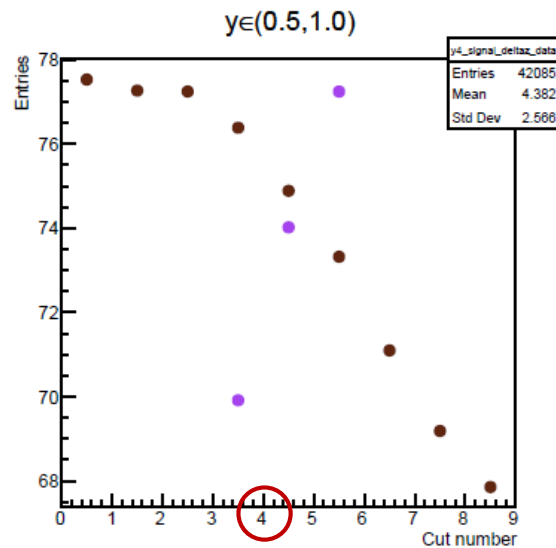
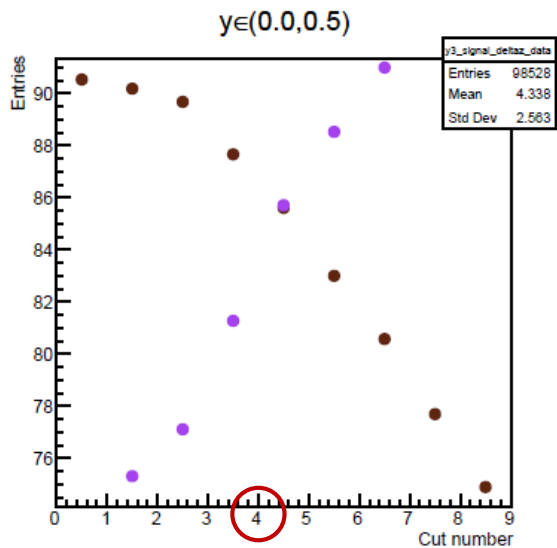
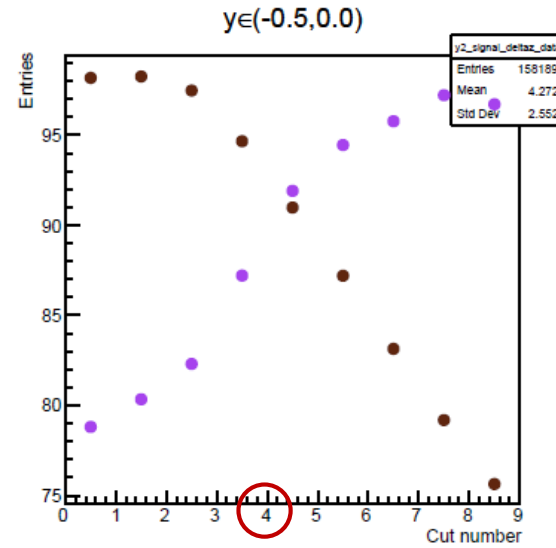
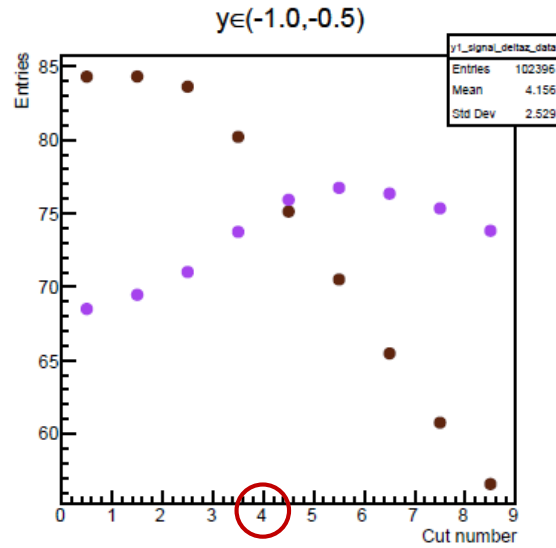
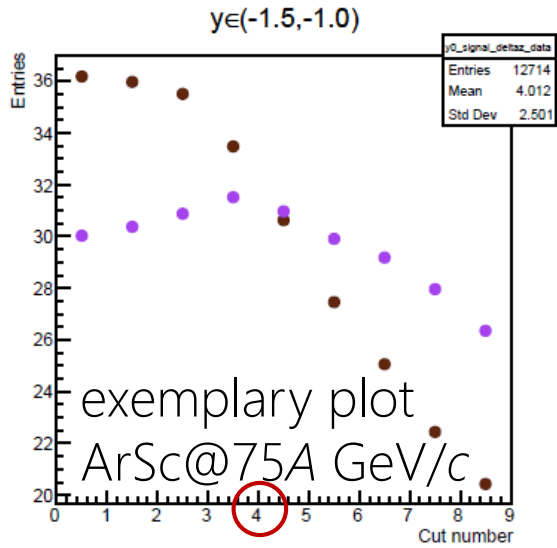
Stability plots for DirA selection



Cut number	DirA value
1	0.99
2	0.995
3	0.999
4	0.9995
5	0.9999
6	0.99995
7	0.99999
8	0.999995

$$N_{corr} = N_{raw} \cdot \frac{N_{gen}}{N_{acc}}$$

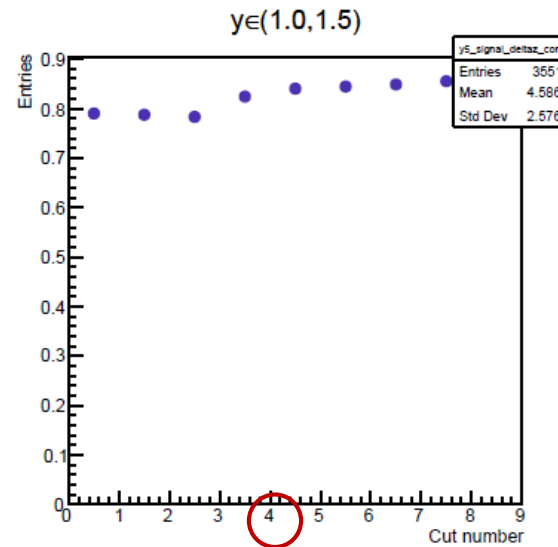
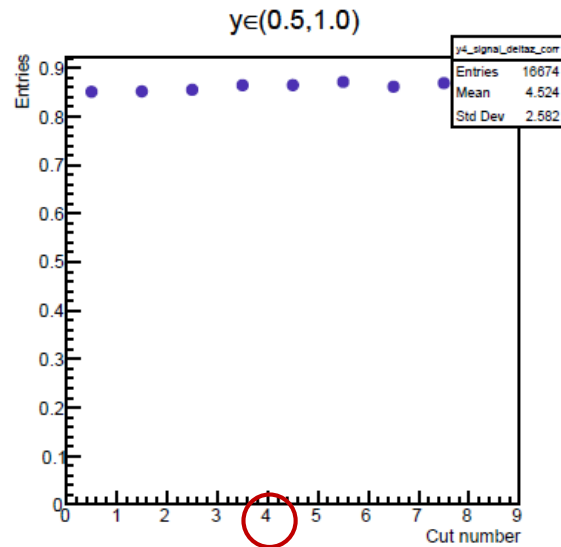
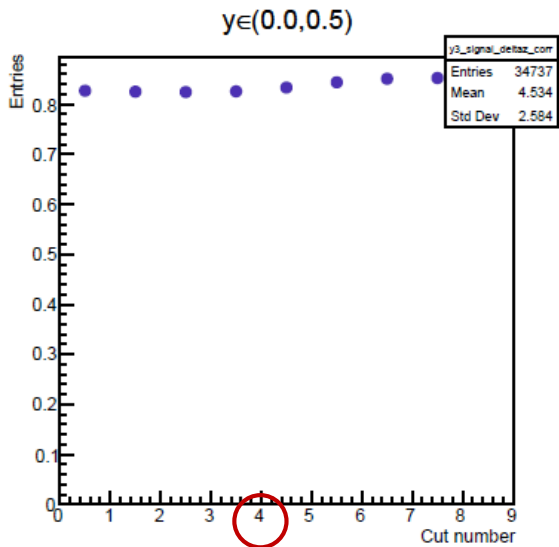
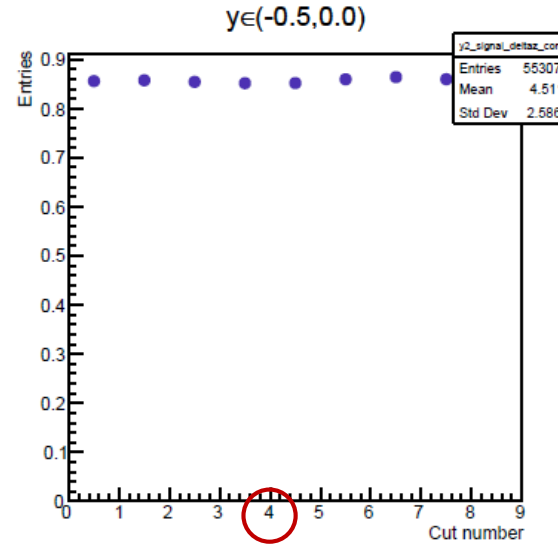
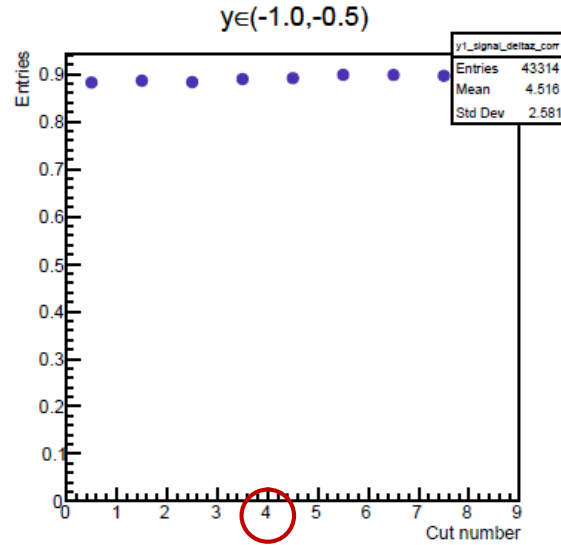
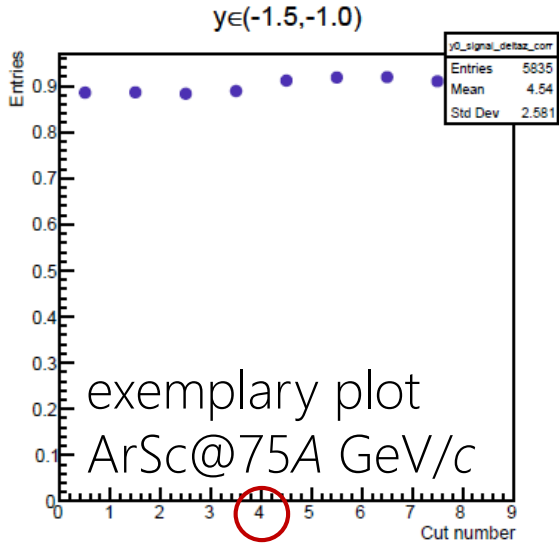
Signal significance for ΔL selection



Cut number	deltaL value
1	2.5
2	5
3	7.5
4	10
5	12.5
6	15
7	17.5
8	20

$$SS = \frac{S_{sim}}{\sqrt{S_{sim} + B_{sim}}}$$

Stability plots for ΔL selection

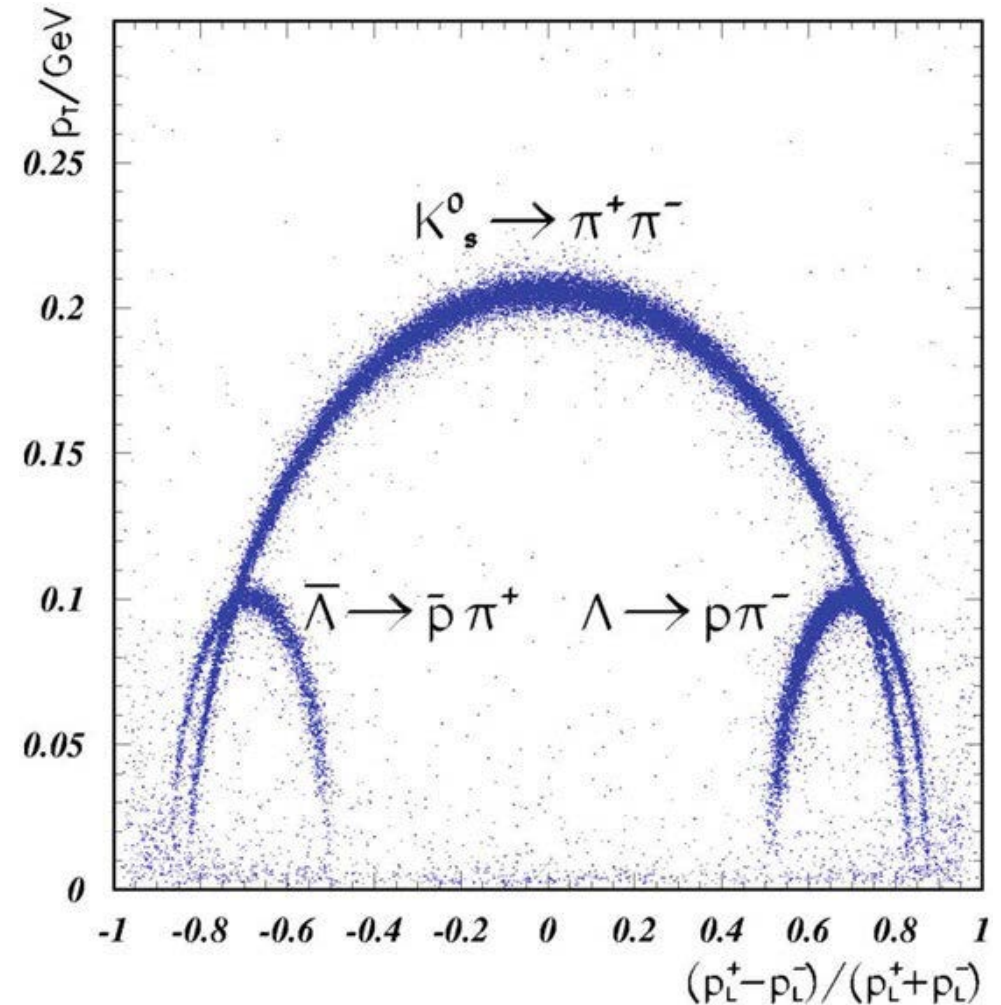


Cut number	deltaL value
1	2.5
2	5
3	7.5
4	10
5	12.5
6	15
7	17.5
8	20

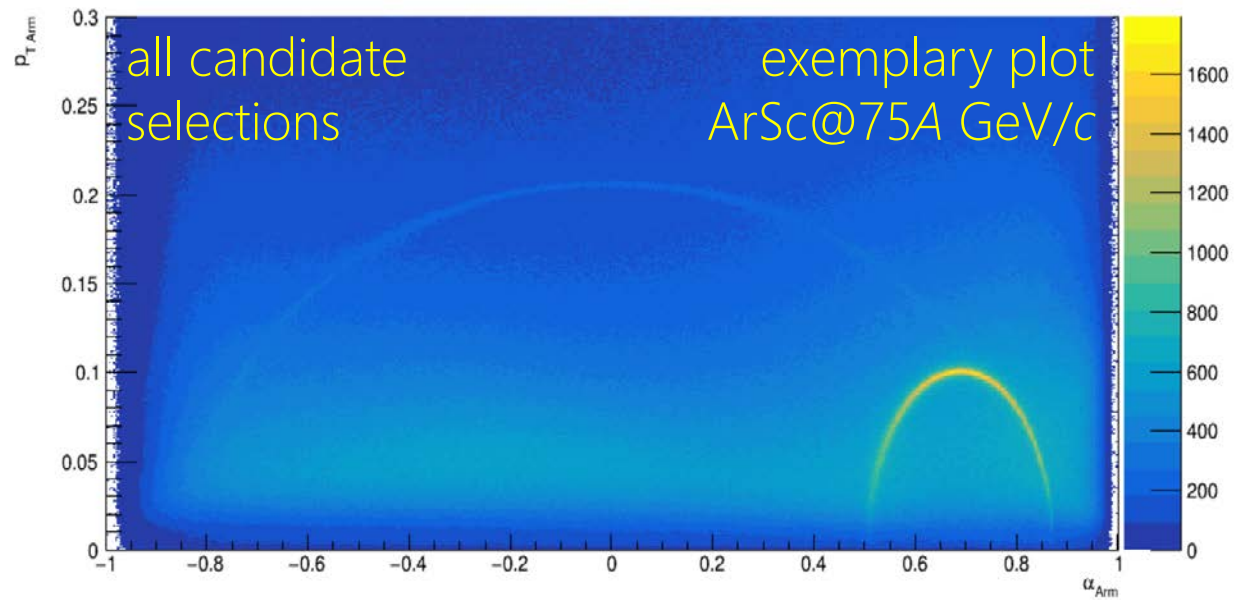
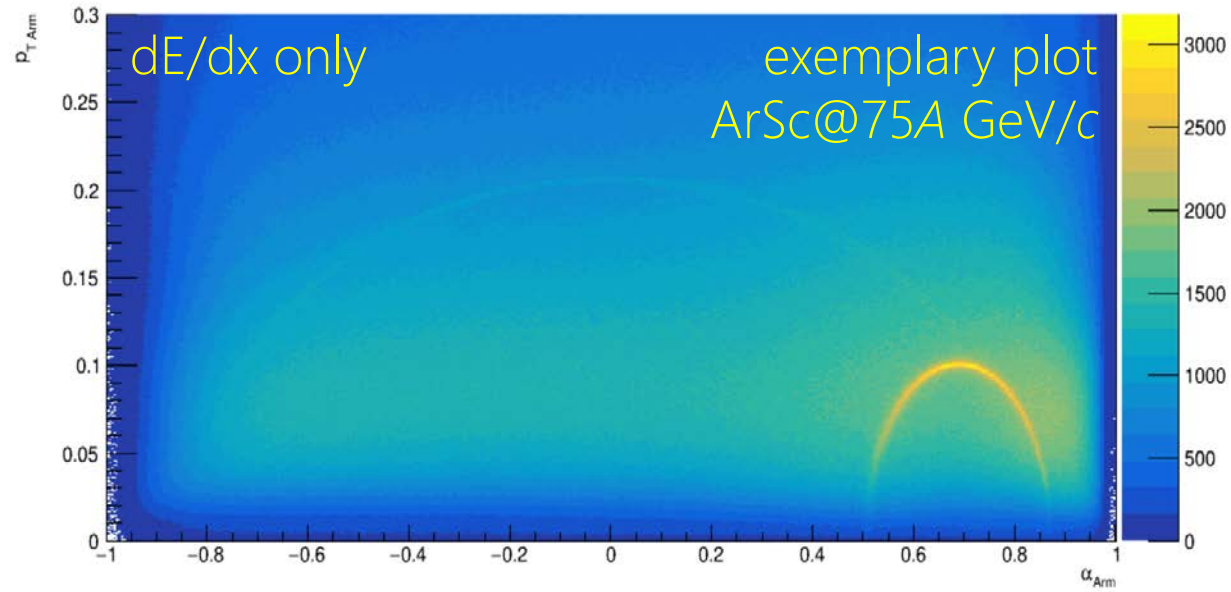
$$N_{corr} = N_{raw} \cdot \frac{N_{gen}}{N_{acc}}$$

Armenteros-Podolanski plot as analysis quality check

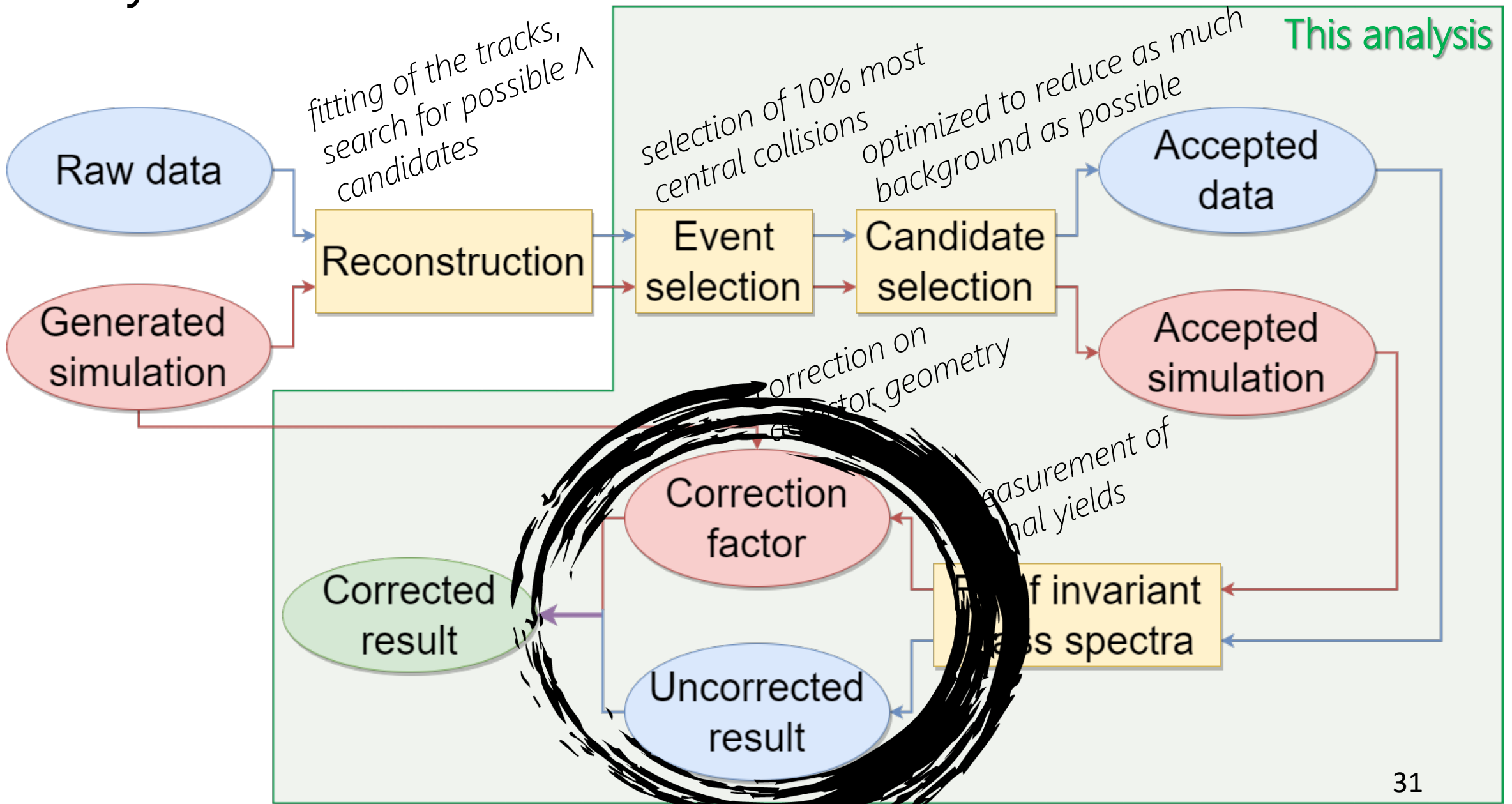
- a two-dimensional plot of transverse momentum p_T of the decay products with respect to the mother particle versus the longitudinal momentum asymmetry $\alpha = \frac{p_L^+ - p_L^-}{p_L^+ + p_L^-}$
- the decay products of K_S^0 have the same mass, so their momenta are distributed **symmetrically** on average
- for Λ ($\bar{\Lambda}$) decays the proton (antiproton) takes on average a larger part of the momentum, so the distribution is **asymmetric**



Armenteros-Podolanski plot as analysis quality check

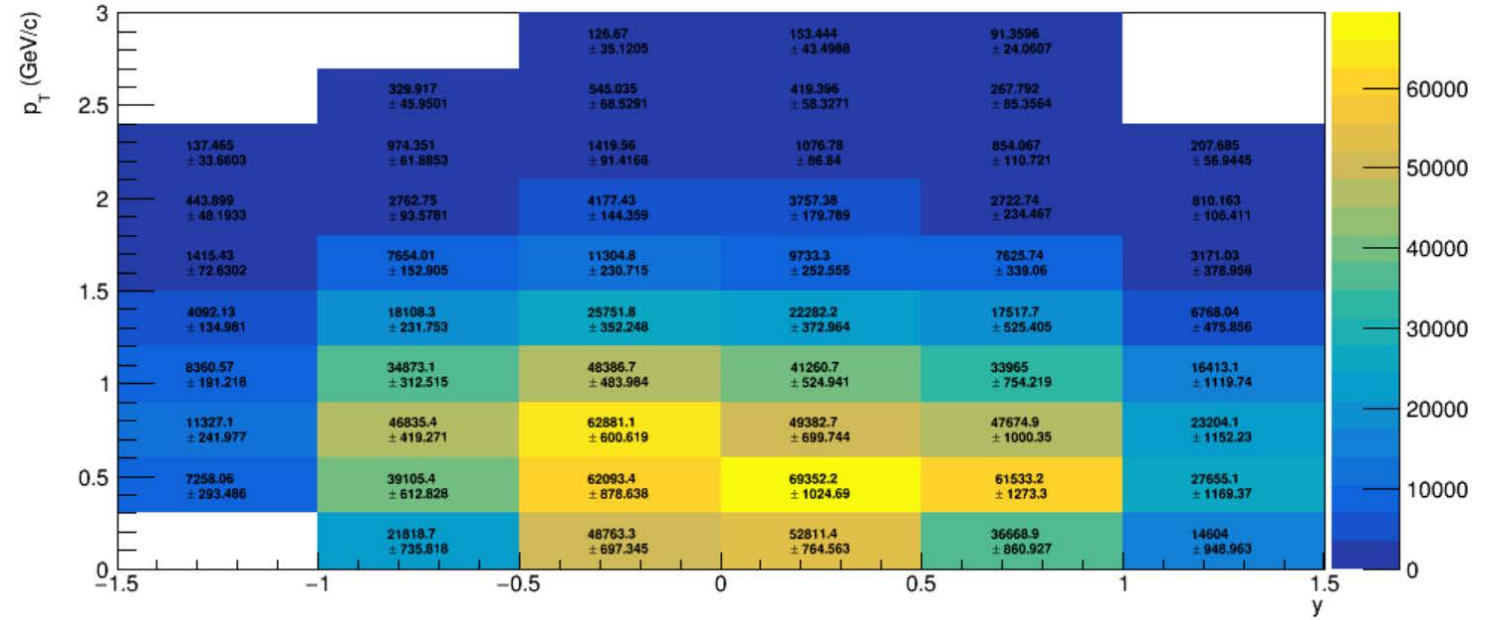


Analysis workflow

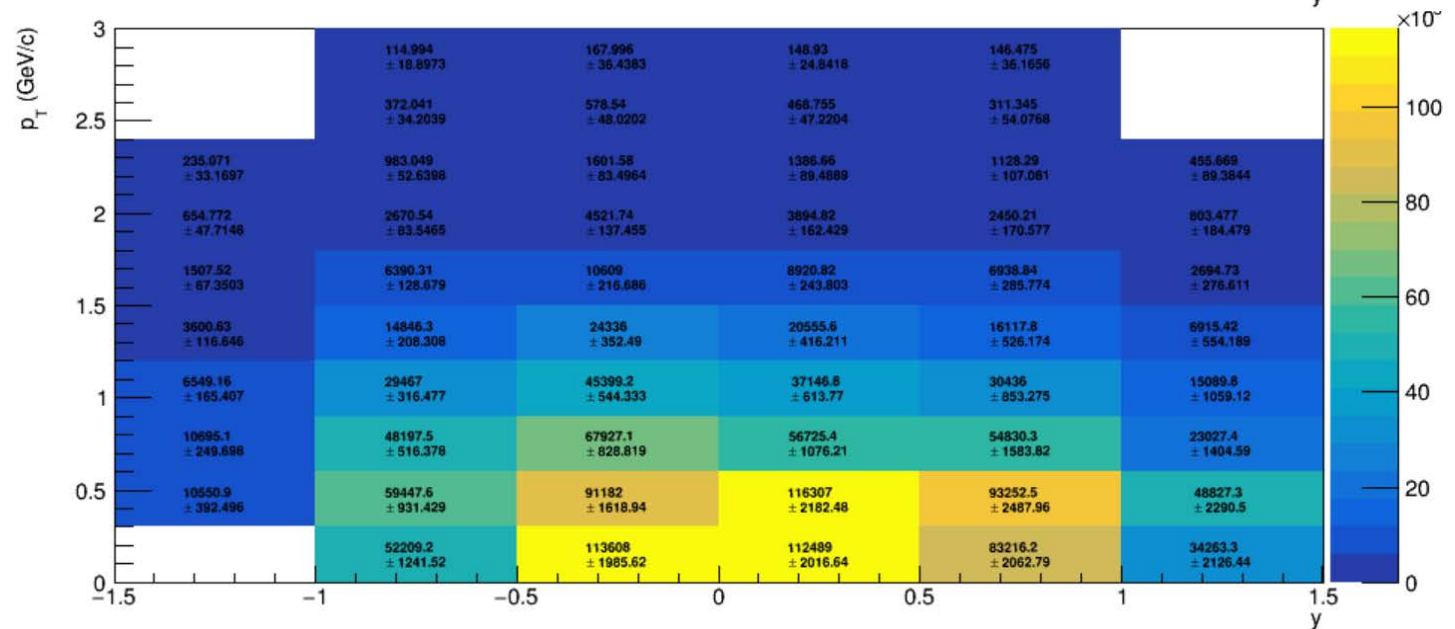


Uncorrected spectra

uncorrected
data



uncorrected
simulation



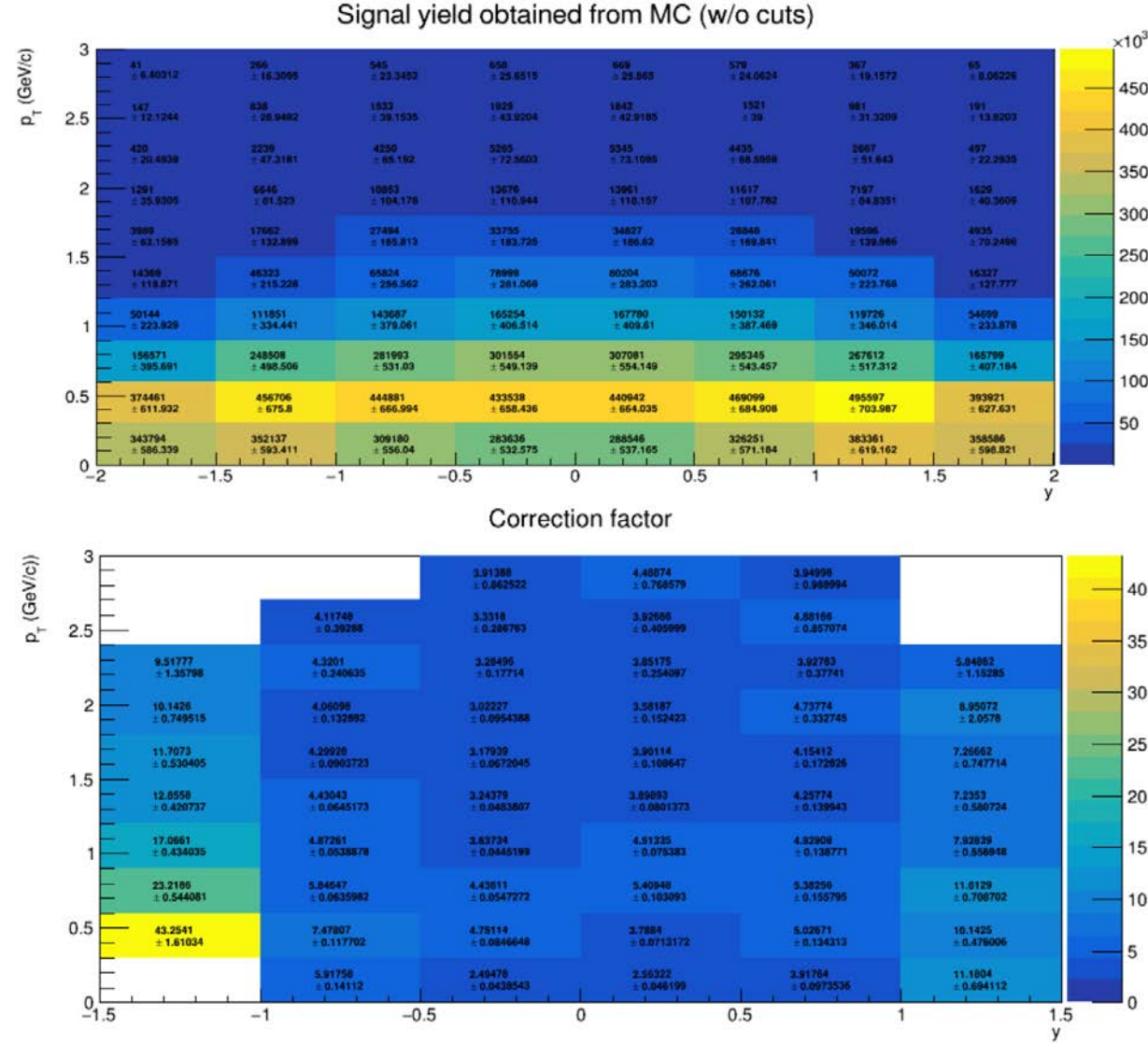
Correction factor

- based on a detailed Monte Carlo simulation,
- is calculated to correct for losses due to the trigger bias, geometrical acceptance, reconstruction efficiency, and the selection criteria applied in the analysis:

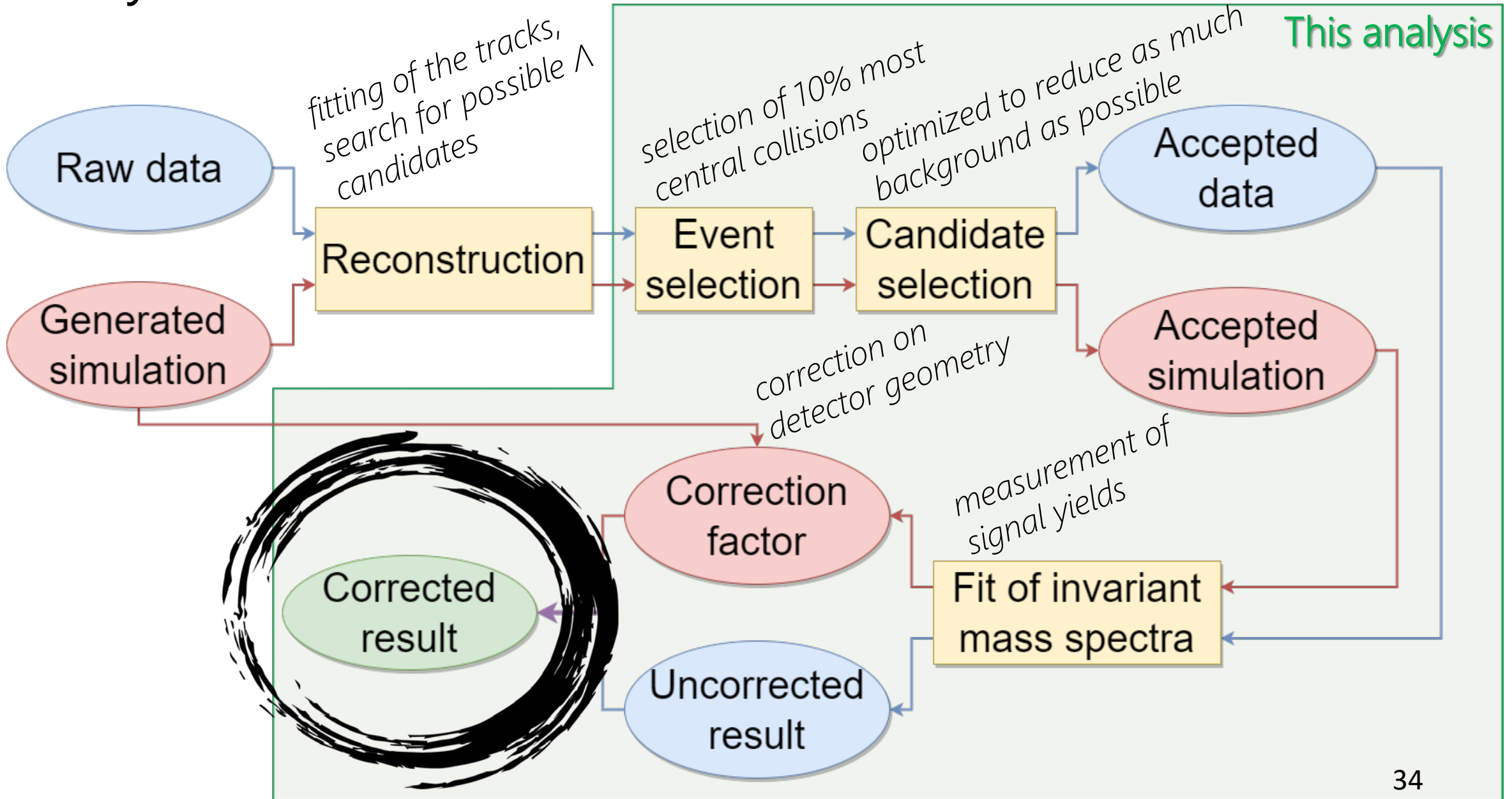
$$c_{MC}(y, p_T) = \frac{n_{MC}^{gen}(y, p_T)}{N_{MC}^{gen}} \bigg/ \frac{n_{MC}^{acc}(y, p_T)}{N_{MC}^{acc}}$$

- additionally, loss of the Λ baryons due to the dE/dx selection is also corrected with a factor:

$$c_{dE/dx} = \frac{1}{\epsilon^2} = 1.005$$



Analysis workflow

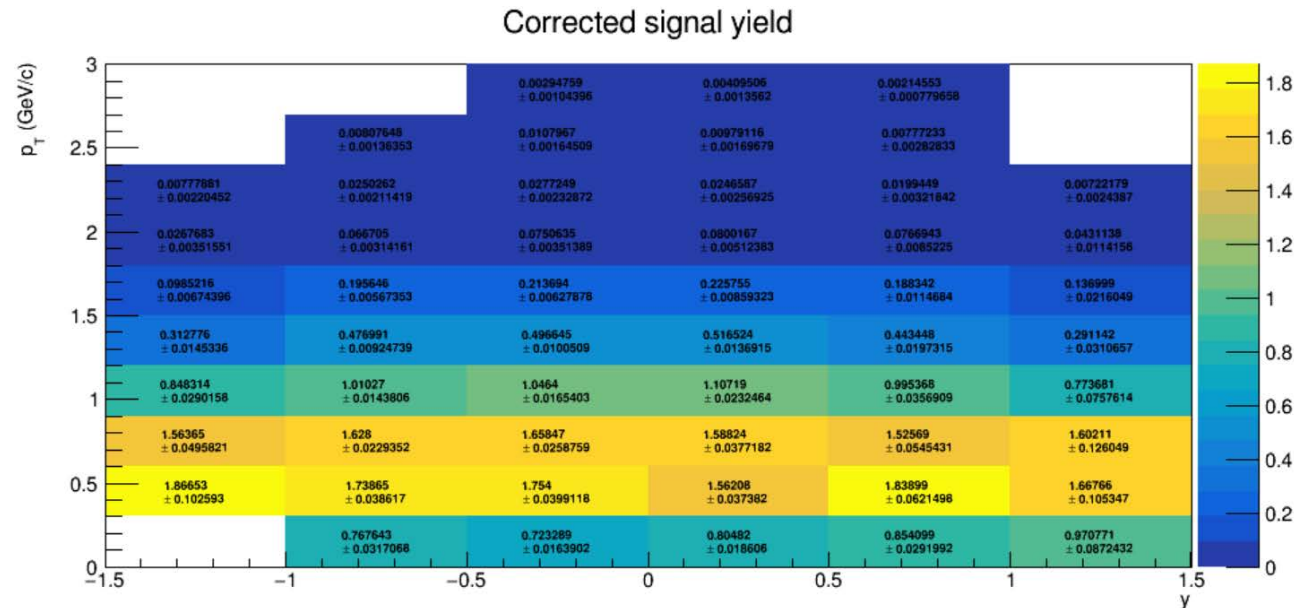


Double-differential yields and statistical uncertainties

- double-differential yield of Λ baryons per inelastic event in a given bin is calculated as follows:

$$\frac{d^2n}{dydp_T}(y, p_T) = \frac{c_{dE/dx} \cdot c_{MC}(y, p_T)}{\Delta y \Delta p_T} \cdot \frac{n_{\Lambda}(y, p_T)}{N_{events}}$$

- statistical uncertainties receive contributions from the statistical uncertainty of the correction factor and the statistical uncertainty of the uncorrected number of Λ



Systematic uncertainties

Four possible groups of systematic uncertainty sources are related to

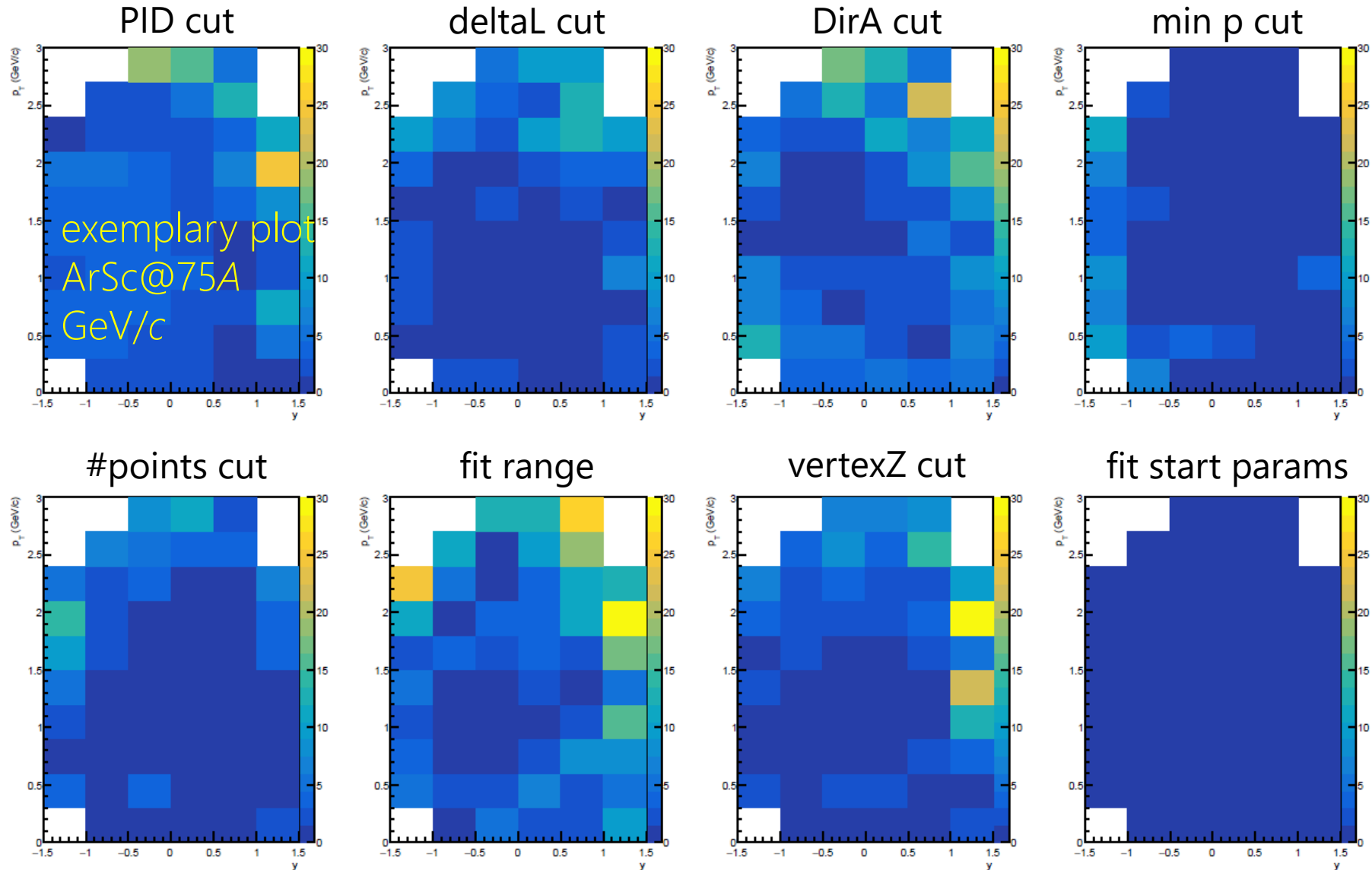
- event selection criteria,
- track selection criteria,
- candidate selection criteria,
- signal extraction procedure.

The procedure of total systematic uncertainty in a given bin is following:

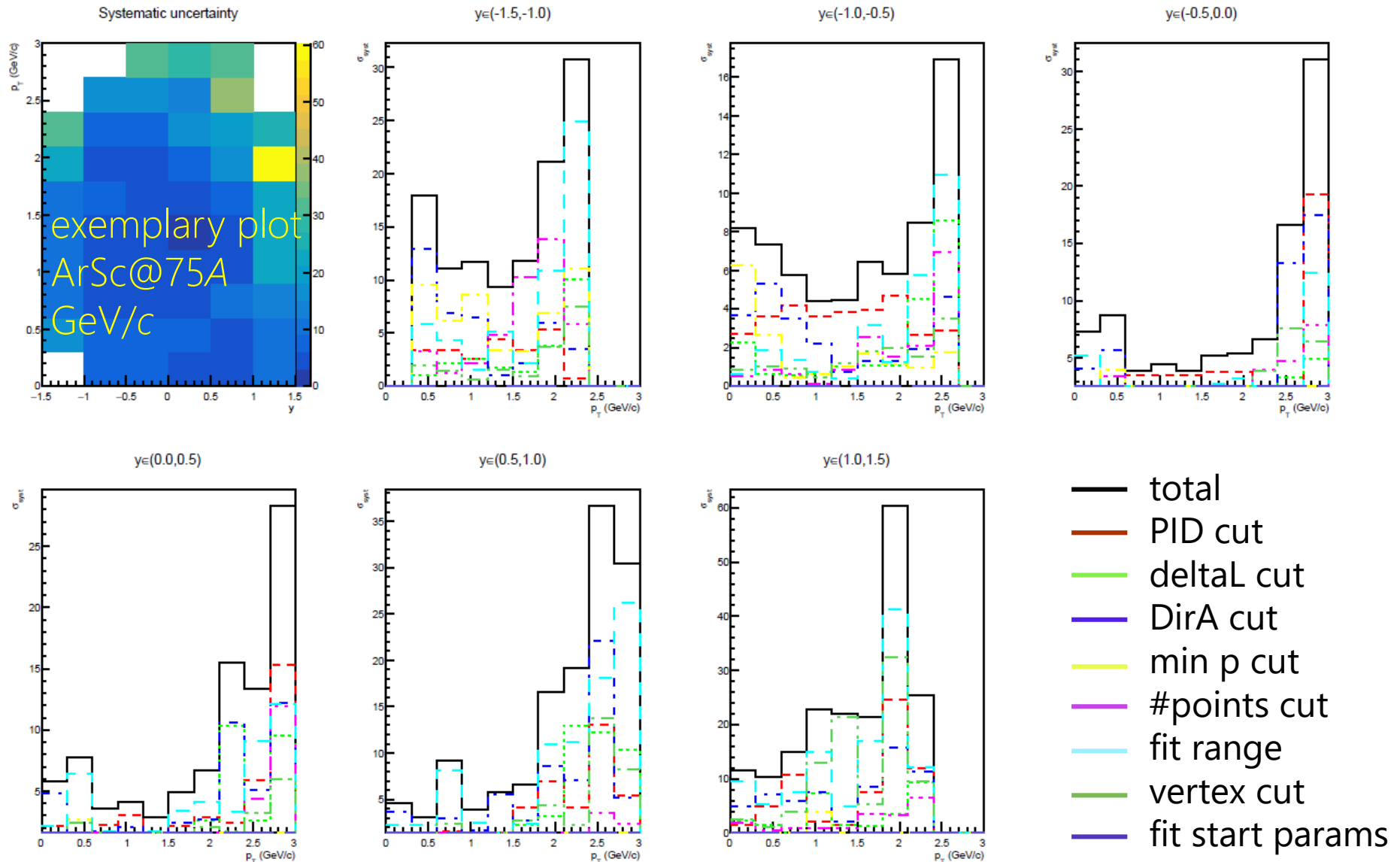
- each selection is changed to its tighter and looser version
- maximum deviations are determined for every selection, which contributes to the systematic uncertainty
- total uncertainty is calculated as the sum in quadrature.

Systematic uncertainties - contributions

$$\sigma_{sys}[\%] = \frac{|N_{mod} - N_{base}|}{N_{base}} \times 100 [\%]$$

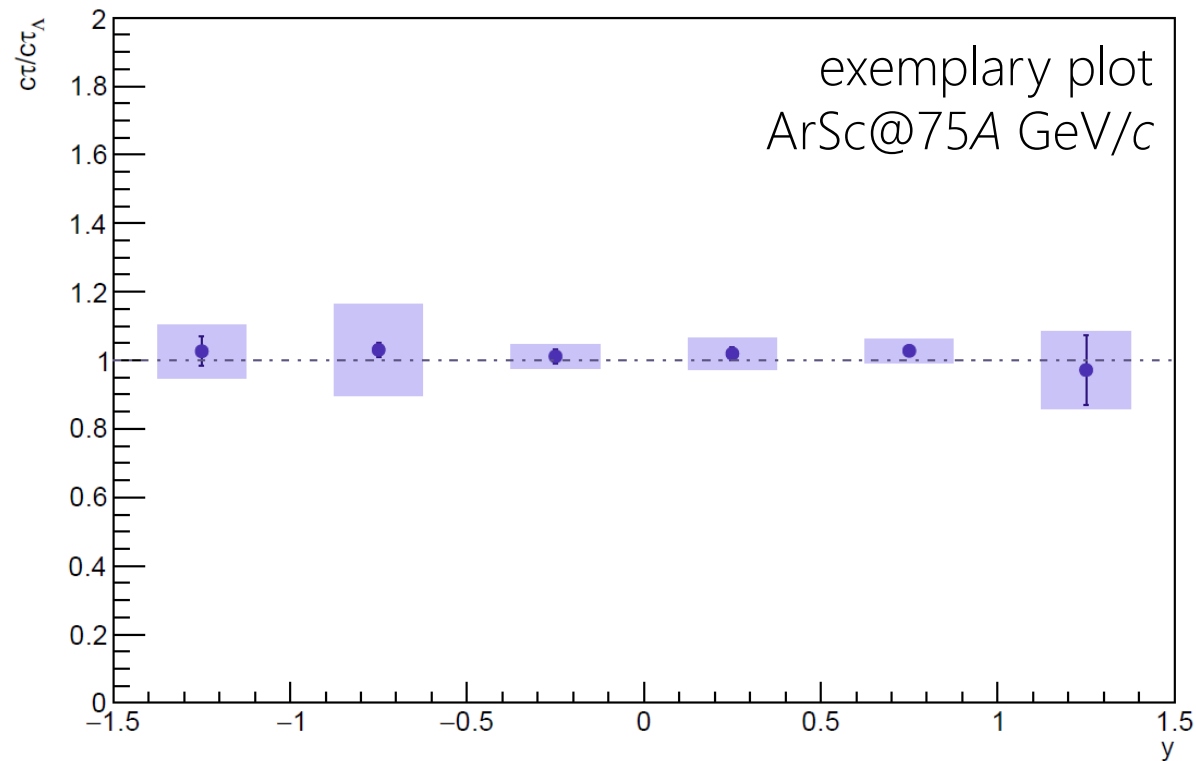


Total systematic uncertainties

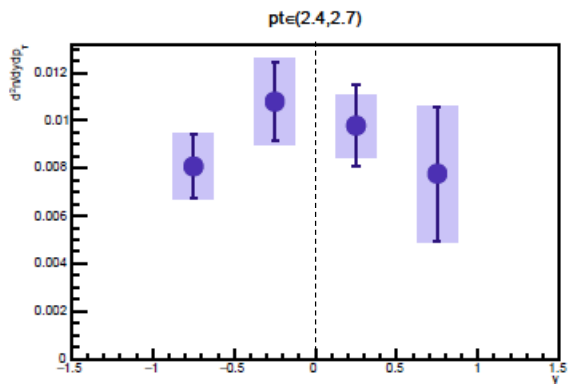
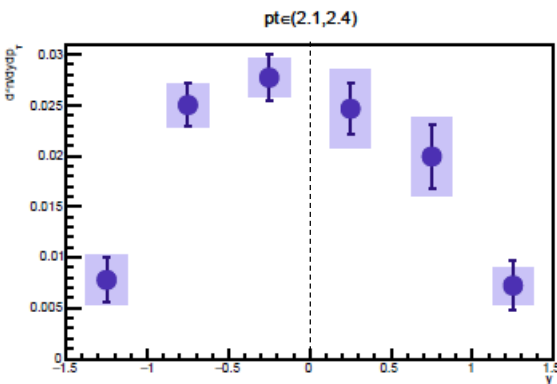
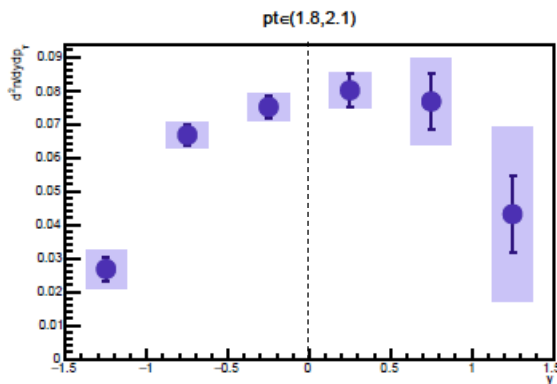
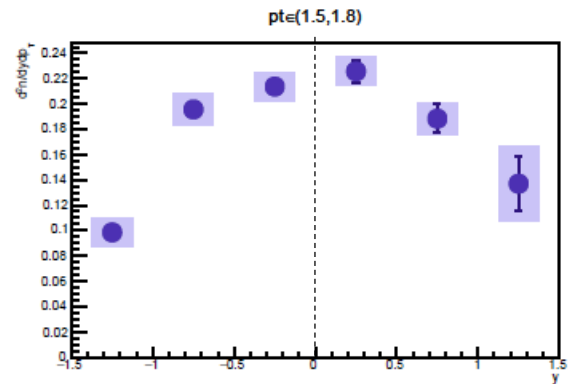
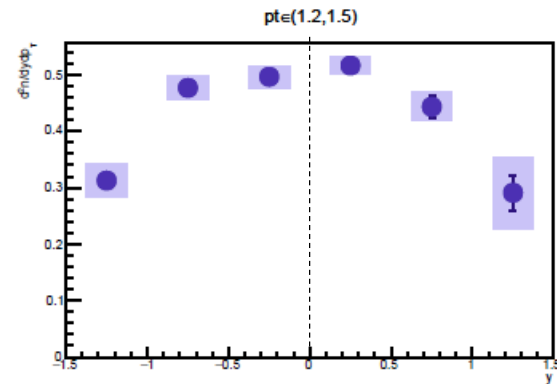
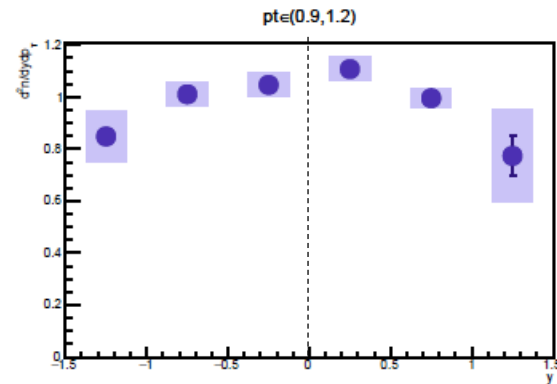
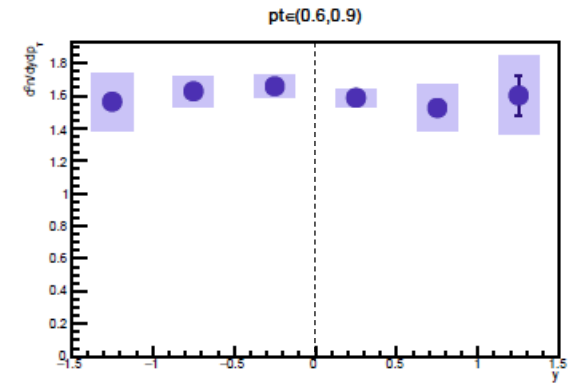
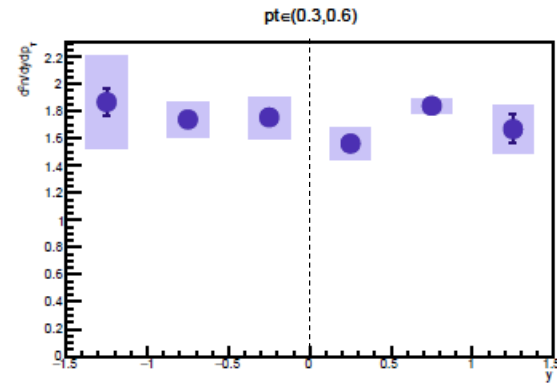
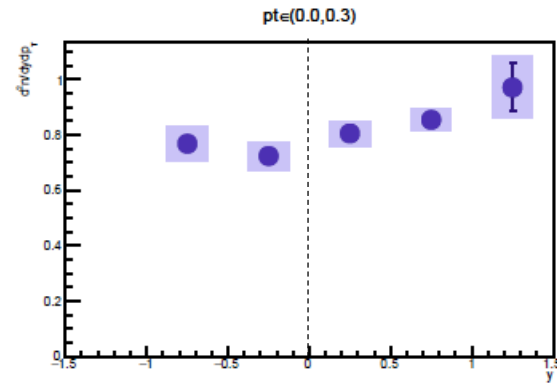


Lifetime distributions as analysis quality check

- reliability of the reconstruction and of the correction procedure can be validated by studying the lifetime distribution of candidates
- lifetime of each candidate is calculated from the candidate's path length and velocity
- lifetime distributions are fitted by an exponential distribution to obtain proper lifetimes
- measured mean lifetime is compared to the PDG value $c\tau_{\Lambda} = 7.89$ cm

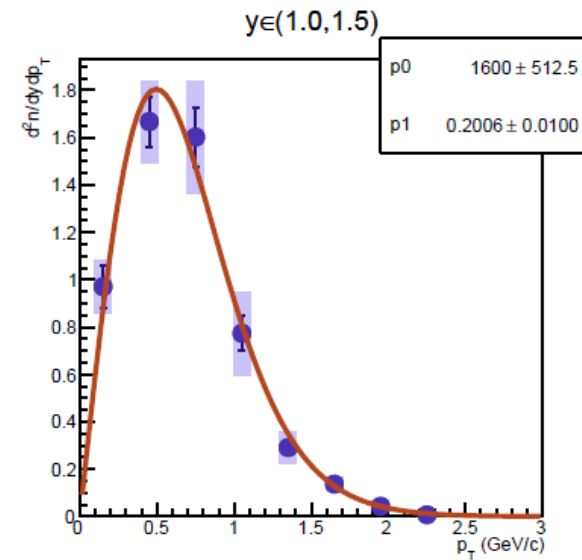
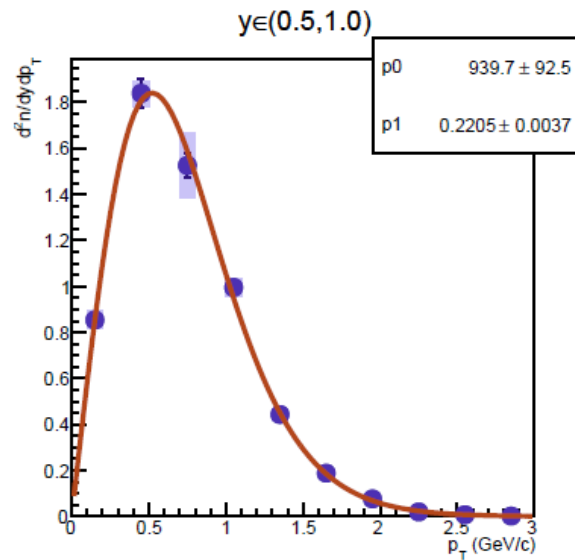
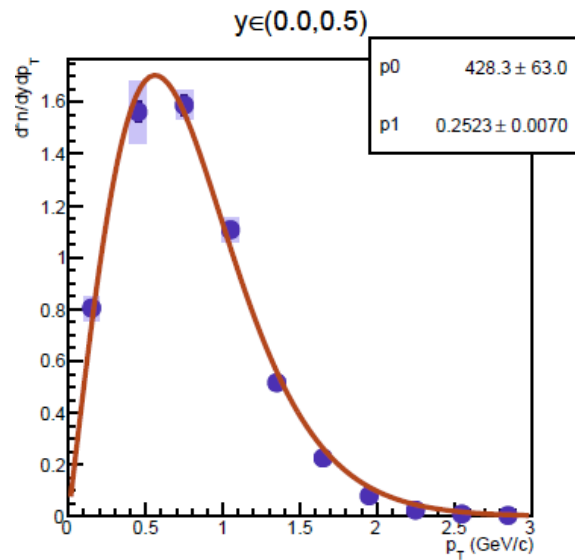
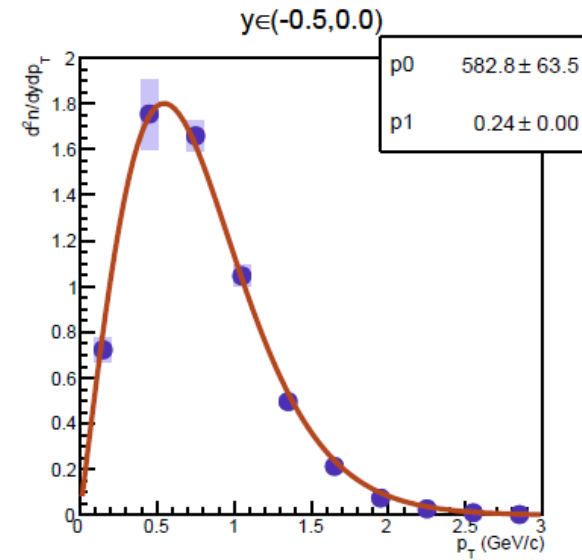
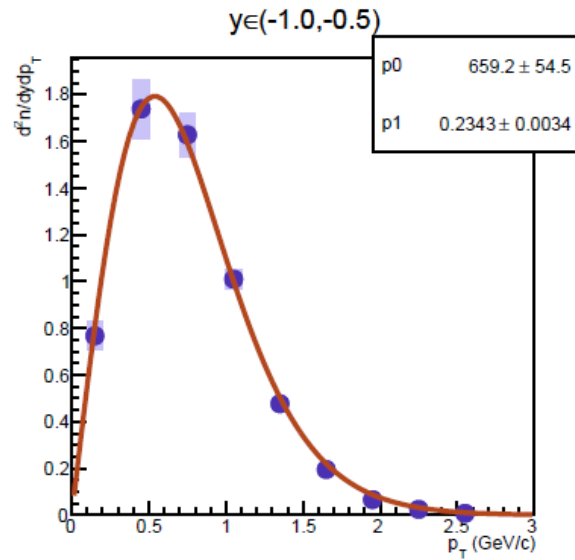
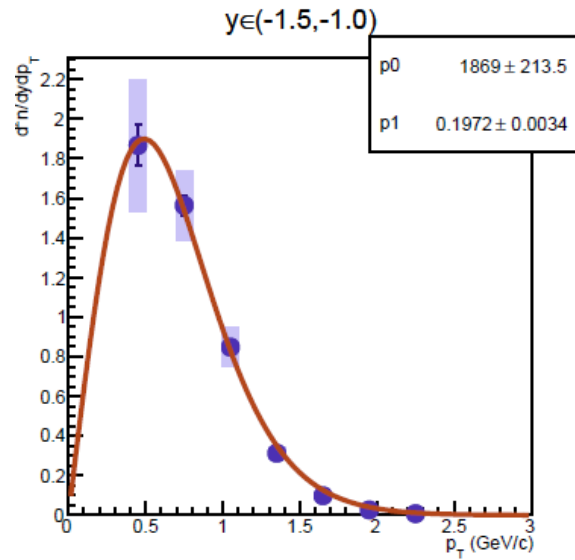


Rapidity distributions

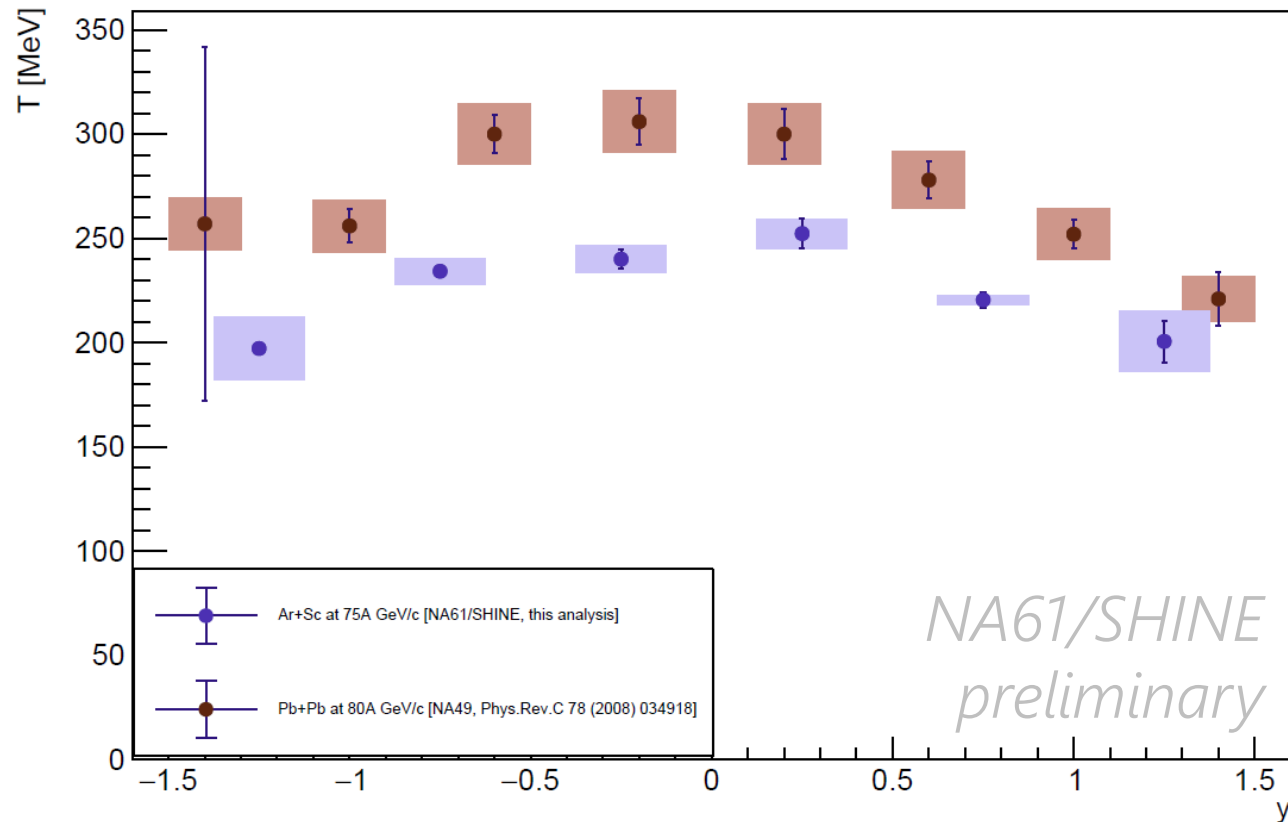


Transverse momentum distributions

$$f(p_T) = A \cdot p_T \cdot \exp\left(\frac{\sqrt{p_T^2 + m_0^2}}{T}\right)$$



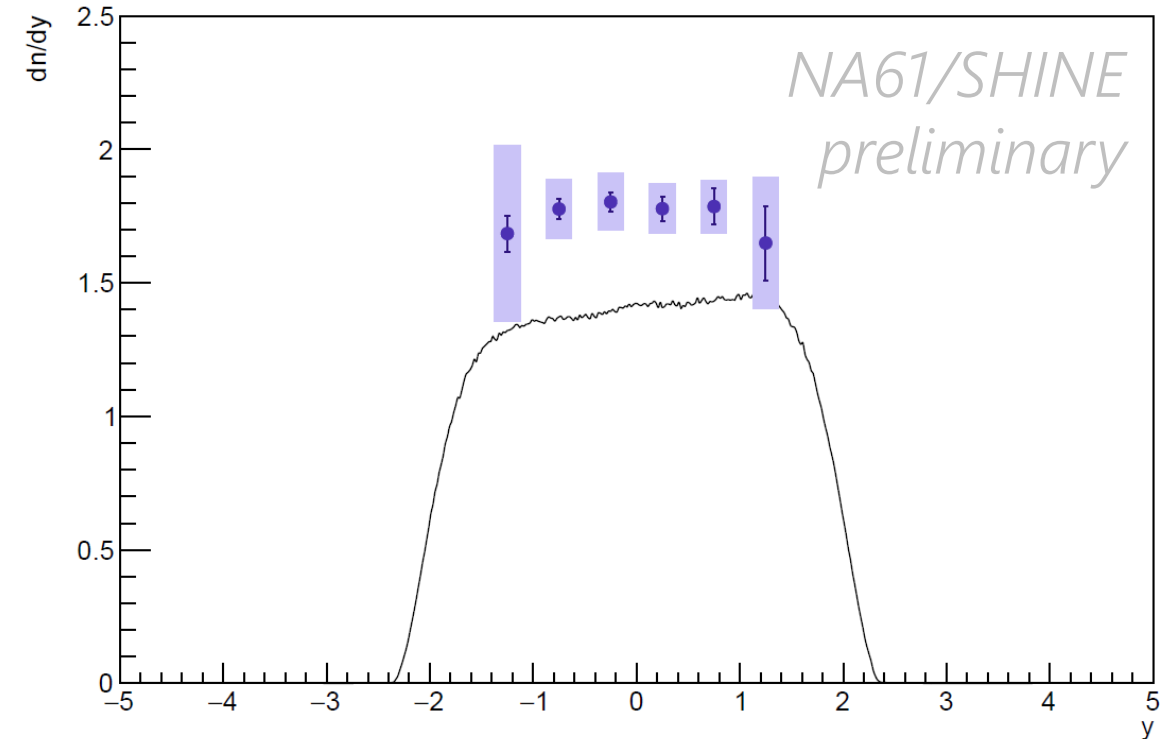
Inverse slope parameter distribution: NA61/SHINE ArSc vs. NA49 PbPb



- the inverse slope parameter (effective temperature) is systematically **lower** for ArSc than for PbPb, though **close** to it

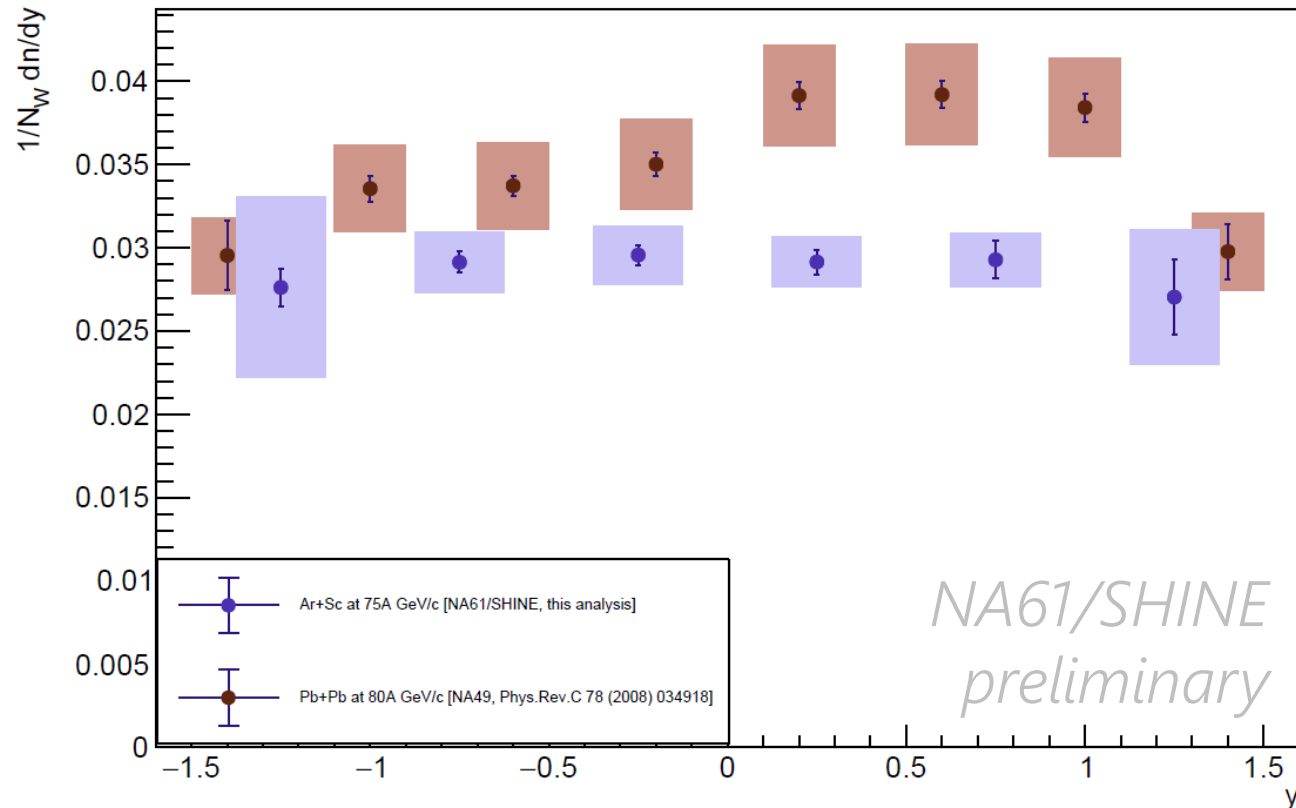
dn/dy distribution: **data** vs. EPOS

- mean multiplicity is calculated as the sum of measured points scaled under the assumption that the ratio between measured and unmeasured regions is the same in data and MC
- statistical uncertainty is calculated as the sum of points' statistical error and integral error from fitted function in an unmeasured region
- systematic uncertainty is estimated as the sum of systematic uncertainty and half of the extrapolated integral
 - the EPOS1.99 model **underestimates** yields by 20-25%



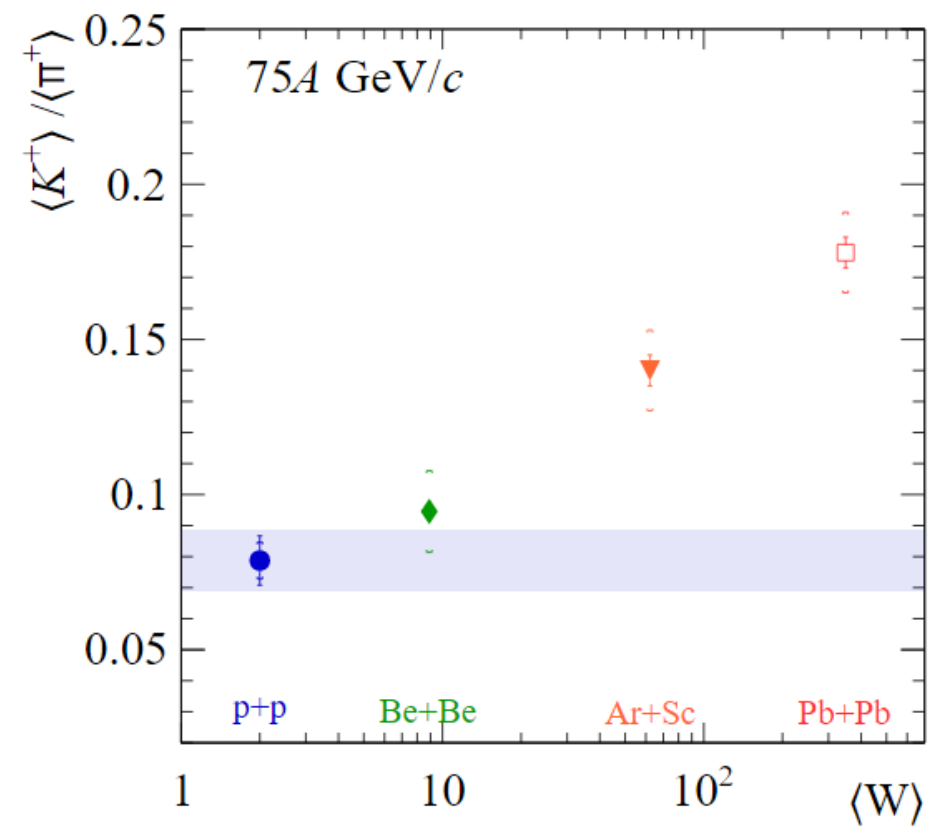
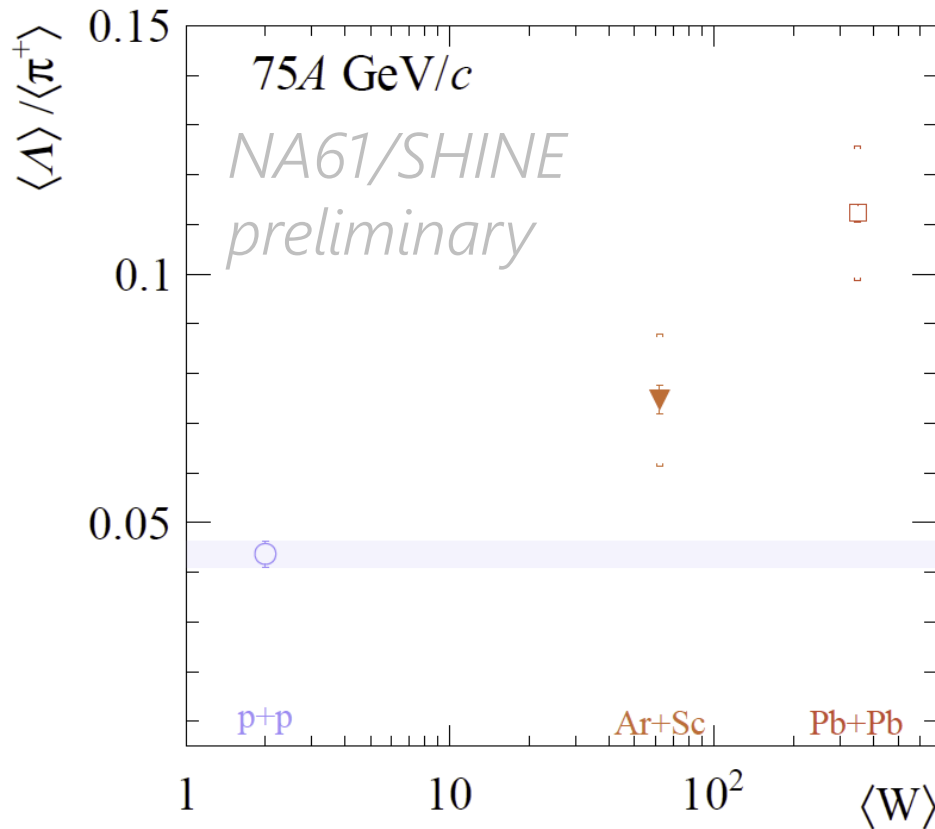
$$\langle \Lambda \rangle = 6.44 \pm 0.24 (stat) \pm 1.10 (syst)$$

dn/dy distribution: NA61/SHINE ArSc vs. NA49 PbPb



- the yields scaled by number of the wounded nucleons are systematically **lower** for ArSc than for PbPb

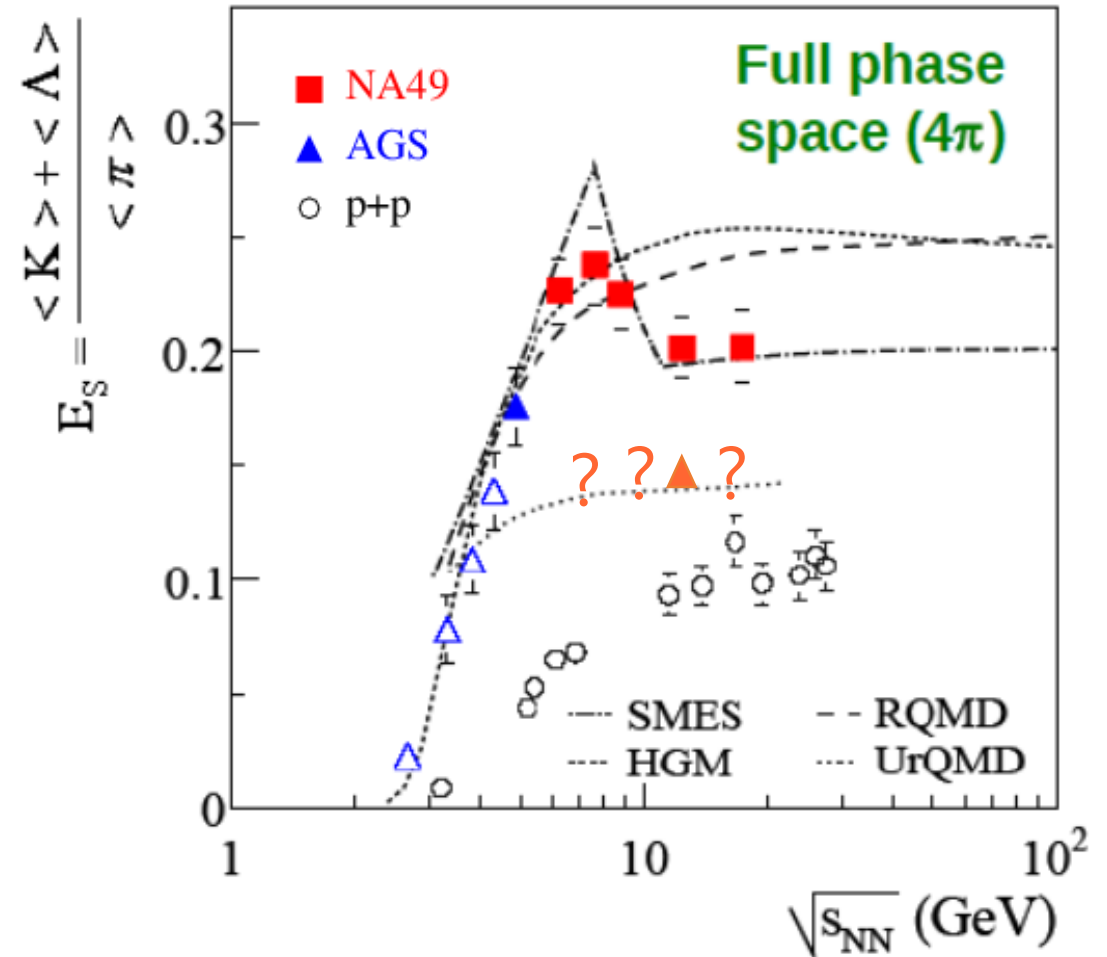
System size dependence of $\langle \Lambda \rangle / \langle \pi^+ \rangle$ and $\langle K^+ \rangle / \langle \pi^+ \rangle$ ratios



➤ $\langle \Lambda \rangle / \langle \pi^+ \rangle$ ratio shows qualitatively similar trend to that of $\langle K^+ \rangle / \langle \pi^+ \rangle$ ratio

Instead of conclusions

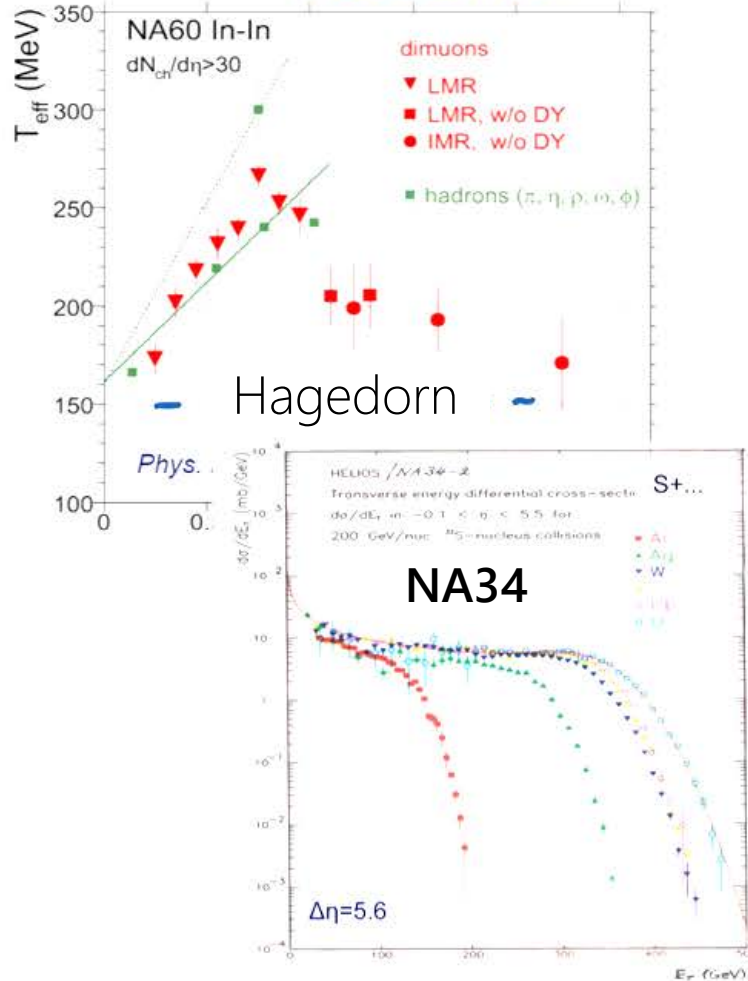
- Λ analysis for Ar+Sc@75A GeV/c is concluded and preliminary released
- Λ analysis for Ar+Sc@40A GeV/c and Ar+Sc@150A GeV/c are ongoing and to be preliminary released soon
- exciting times for exploring strangeness ahead



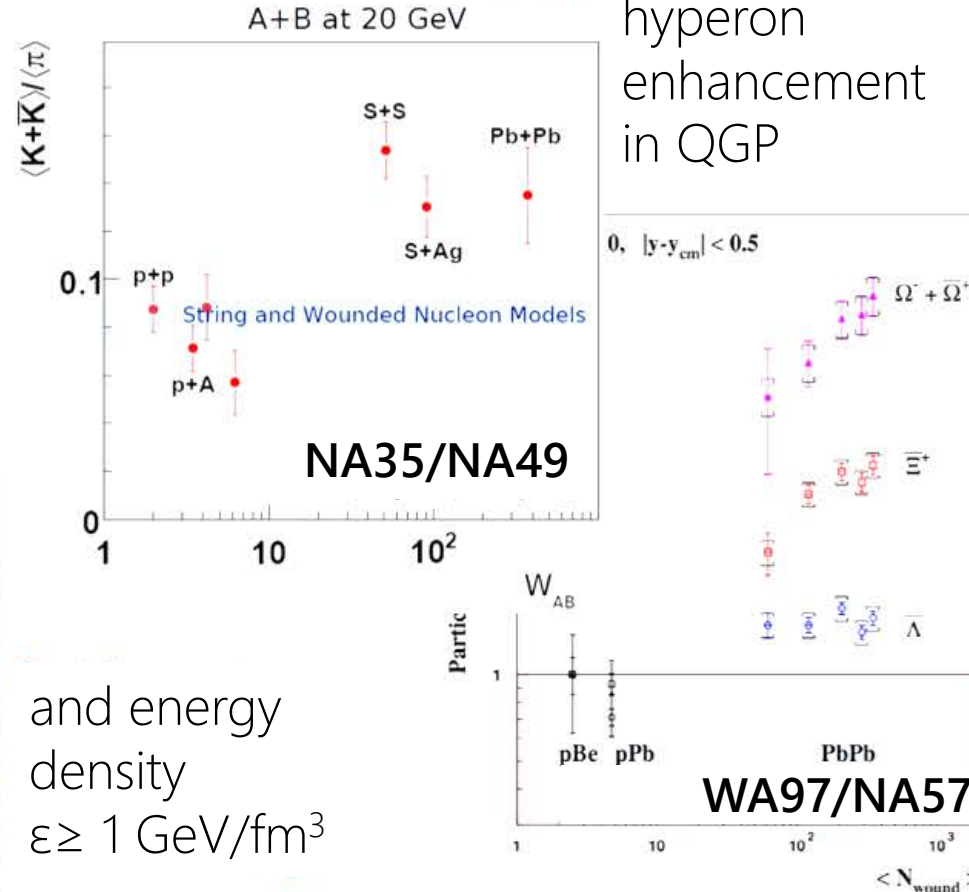
Backup

Quark-gluon plasma: signatures

QGP temperature
 $T \approx 200$ MeV

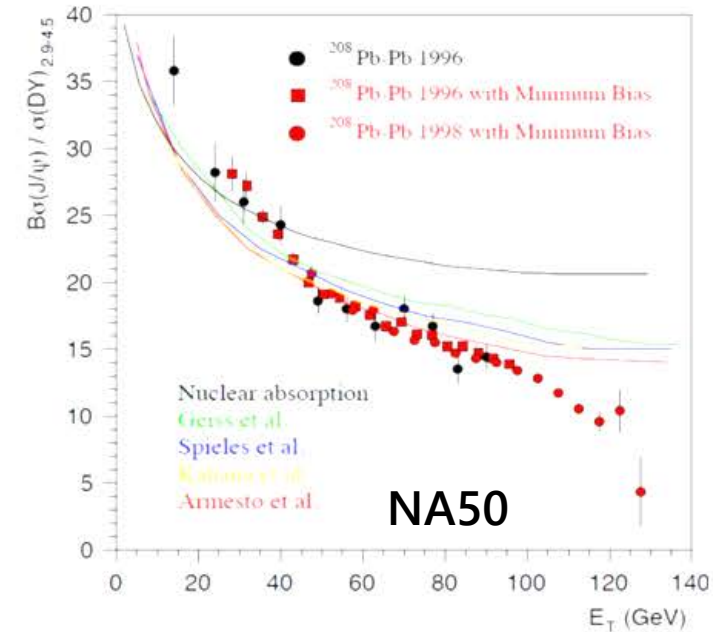


Strangeness and multi-strange hyperon enhancement in QGP



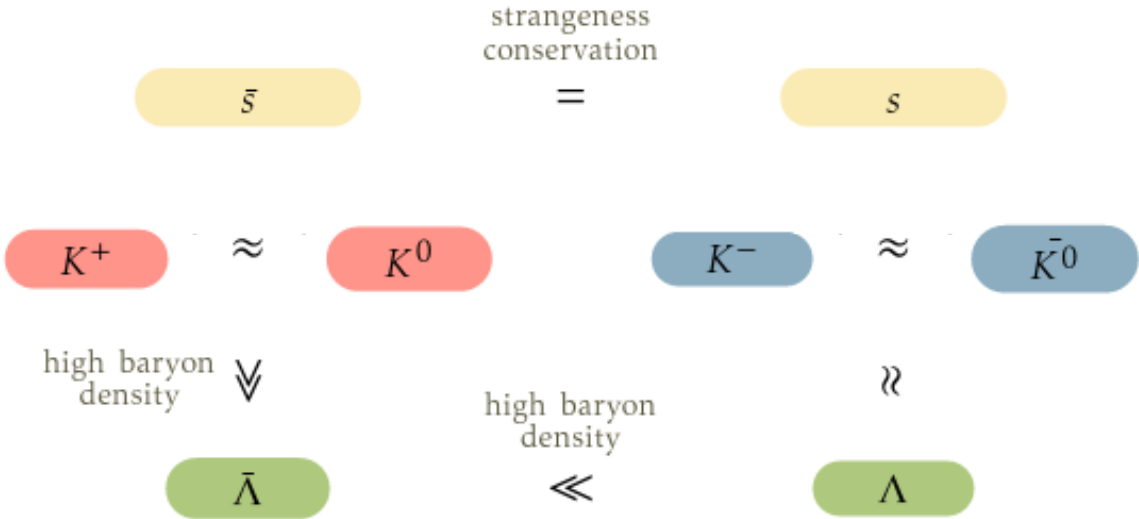
and energy density
 $\epsilon \geq 1$ GeV/fm³

J/ψ melting in QGP



M. Gazdzicki, seminar of
 Bogolyubov Institute of
 Theoretical Physics

Main strangeness carriers in A+A collisions at high μ_B



- sensitive to strangeness content only
- sensitive to strangeness content and baryon density

$$\begin{aligned}
 p + p &\rightarrow p + \Lambda + K^+ + \pi^0 && \approx [\text{GeV}] 0.94 + 0.94 \rightarrow 0.94 + 1.12 + 0.49 + 0.14 \\
 p + p &\rightarrow p + p + K^+ + K^- && \approx [\text{GeV}] 0.94 + 0.94 \rightarrow 0.94 + 0.94 + 0.49 + 0.49
 \end{aligned}$$

The first option is almost 200MeV "cheaper".

Strange definitions

Strangeness production $\langle N_{s\bar{s}} \rangle$ – number of $s\bar{s}$ pairs produced in a collision.

$$\begin{aligned}2 \cdot \langle N_{s\bar{s}} \rangle &= \langle \Lambda + \bar{\Lambda} \rangle + \langle K + \bar{K} \rangle + \langle \phi \rangle + \dots \\2 \cdot \langle N_{s\bar{s}} \rangle &\approx \langle \Lambda \rangle + \langle K^+ + K^- + K^0 + \bar{K}^0 \rangle\end{aligned}$$

Entropy production $\propto \langle \pi \rangle$

The experimental ratio of strangeness to entropy can be defined as:

$$E_S = \frac{\langle \Lambda \rangle + \langle K + \bar{K} \rangle}{\langle \pi \rangle} \approx \frac{2 \cdot \langle N_{s\bar{s}} \rangle}{\langle \pi \rangle}$$

$$\langle N_{s\bar{s}} \rangle \approx \langle K^+ \rangle + \langle K^0 \rangle \approx 2 \cdot \langle K^+ \rangle, \quad \langle \pi \rangle \approx \frac{3}{2} (\langle \pi^+ \rangle + \langle \pi^- \rangle)$$

$$\frac{\langle N_{s\bar{s}} \rangle}{\langle \pi \rangle} \approx \frac{2 \langle K^+ \rangle}{3 \langle \pi^+ \rangle}, \quad E_S \approx \frac{4 \langle K^+ \rangle}{3 \langle \pi^+ \rangle}$$

Strangeness enhancement E_S in Ar+Sc @ 75A GeV/c

- $E_S = \frac{\langle \Lambda \rangle + 4\langle K_S^0 \rangle}{\langle \pi \rangle} = 0.1841 \pm 0.0033 \text{ (stat)} \pm 0.0205 \text{ (syst)}$

using that $\langle \Lambda \rangle = 6.44 \pm 0.24 \pm 1.1$,

$$\langle K_S^0 \rangle = 6.25 \pm 0.09 \pm 0.73,$$

$$\langle \pi^+ \rangle = 86.2 \pm 0.88 \pm 4.23,$$

$$\langle \pi^- \rangle = 84.6 \pm 1.07 \pm 4.31$$

- $E_S = \frac{4\langle K^+ \rangle}{3\langle \pi^+ \rangle} = 0.1856 \pm 0.0090 \text{ (stat)} \pm 0.0294 \text{ (syst)}$

using that $\langle K^+ \rangle = 12 \pm 0.453 \pm 0.695$,

$$\langle \pi^+ \rangle = 86.2 \pm 0.88 \pm 4.23$$

Model comparisons

- ▶ **EPOS** – the reaction proceeds from the excitation of strings according to Gribov-Regge theory to string fragmentation into hadrons.
- ▶ **UrQMD** starts with a hadron cascade based on elementary cross sections for resonance production which either decay (mostly at low energies) or are converted into strings which fragment into hadrons (mostly at high energies).
- ▶ **AMPT** – uses the heavy ion jet interaction generator (HIJING) for generating the initial conditions, Zhang's parton cascade for modeling partonic scatterings and the Lund string fragmentation model or a quark coalescence model for hadronization.
- ▶ **PHSD** is a microscopic offshell transport approach that describes the evolution of a relativistic heavy-ion collision from the initial hard scatterings and string formation through the dynamical deconfinement phase transition to the quark-gluon plasma as well as hadronization and the subsequent interactions in the hadronic phase.
- ▶ **SMASH** uses the hadronic transport approach where the free parameters of the string excitation and decay are tuned to match the experimental measurements in inelastic p+p collisions.

Selection of events in all model calculations follows the procedure for central collisions corresponding to the experimental results (selection based on forward spectator energy).

Event selection - trigger

Name	Definition	Description	Fraction of data
T1	$S1 \cdot S2 \cdot \overline{V1}$	beam	1.16%
T2	$S1 \cdot S2 \cdot \overline{V1} \cdot \overline{S5} \cdot \overline{PSD}$	central interaction	92.61%
T3	$S1 \cdot S2$	beam halo	0.18%
T4	$S1 \cdot S2 \cdot \overline{V1} \cdot \overline{S5}$	min. bias interaction	7.13%

Table 4.2: A list of trigger definitions used during Ar+Sc data taking. The right-most column shows a fraction of data corresponding to an unbiased sample of a given trigger type.

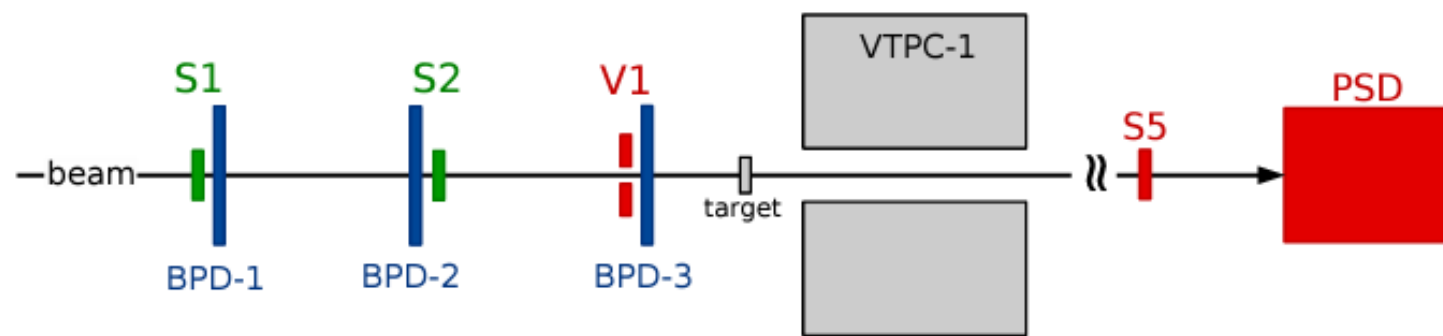
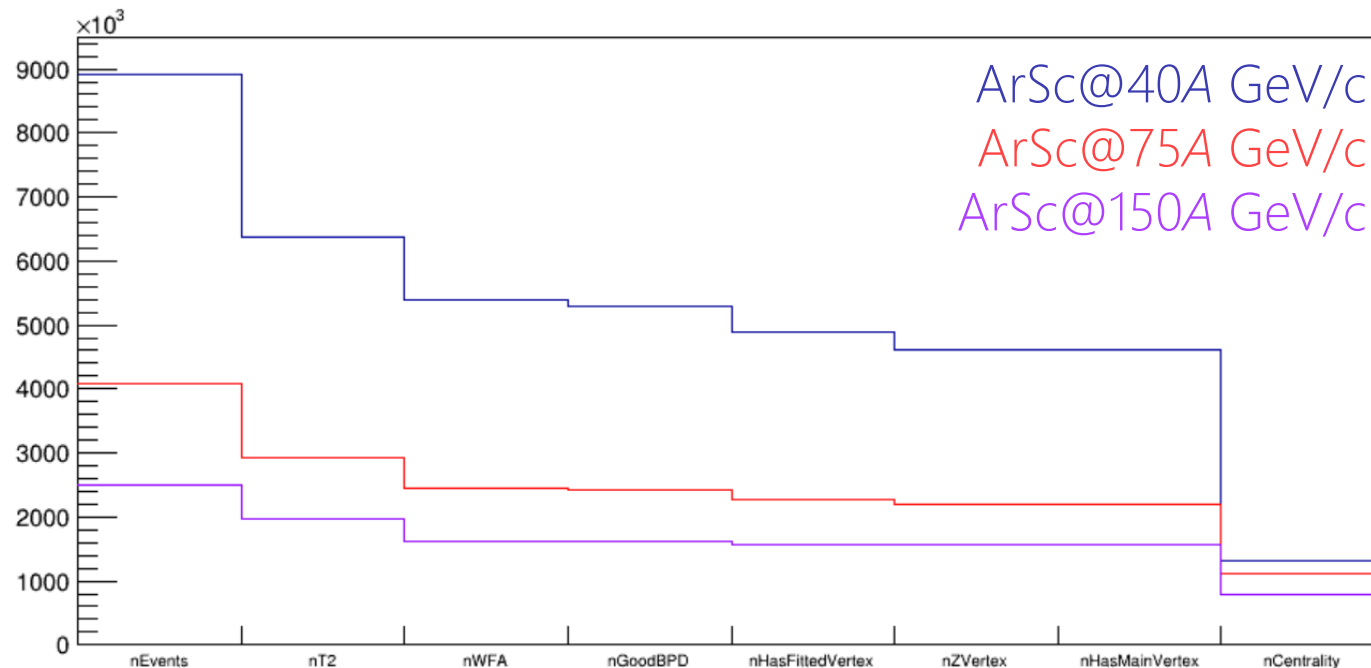


Figure 4.3: A schematic layout of the beam and trigger detectors used during Ar+Sc data taking. Elements working in coincidence mode are marked with green color, the ones working as vetos with red color.

Event selection

Event statistics in experimental data available for the analysis:

P_{beam}	40A GeV/c ($\sqrt{s_{NN}} = 8.77$ GeV)	75A GeV/c ($\sqrt{s_{NN}} = 11.94$ GeV)	150A GeV/c ($\sqrt{s_{NN}} = 16.83$ GeV)
before selection	8.9M events	4.1M events	2.5M events
after selection	1.3M events	1.1M events	0.78M events



System size dependence of $\langle \Lambda \rangle / \langle \pi^- \rangle$ and $\langle K^- \rangle / \langle \pi^- \rangle$ ratios

